(12) LEVEL II

DNA 5131T

HIGH-LATITUDE SCINTILLATION MORPHOLOGY

Alaskan Sector

Stephen J. Matthews
Charles L. Rino
SRI International
333 Ravenswood Avenue
Menlo Park, California 94025

1 October 1979

Topical Report for Period 1 May 1976—1 April 1978

CONTRACT No. DNA 001-77-C-0220

THIS WORK SPONSORED BY THE DEFENSE NUCLEAR AGENCY
UNDER RDT&E RMSS CODE B322078462 I25AAXHX63340 H2590D.

Prepared for
Director
DEFENSE NUCLEAR AGENCY
Washington, D. C. 20305

Destroy this report when it is no longer needed. Do not return to sender.

PLEASE NOTIFY THE DEFENSE NUCLEAR AGENCY, ATTN: STTI, WASHINGTON, D.C. 20305, IF YOUR ADDRESS IS INCORRECT, IF YOU WISH TO BE DELETED FROM THE DISTRIBUTION LIST, OR IF THE ADDRESSEE IS NO LONGER EMPLOYED BY YOUR ORGANIZATION.

UNCLASSIFIED

SECURITY CLASSIFICATION OF THIS PAGE (When Data Entered)

REPORT DOCUMENTATION PAGE

READ INSTRUCTIONS BEFORE COMPLETING FORM

1. REPORT NUMBER: DNA 5131T	2. GOVT ACCESSION NO.: AD-A086222
3. RECIPIENT'S CATALOG NUMBER:	
4. TITLE (and Subtitle): HIGH-LATITUDE SCINTILLATION MORPHOLOGY, Alaskan Sector	5. TYPE OF REPORT & PERIOD COVERED: Topical Report for Period 1 May 76—1 Apr 78
	6. PERFORMING ORG. REPORT NUMBER: SRI Project 6434
7. AUTHOR(s): Stephen J. Matthews, Charles L. Rino	8. CONTRACT OR GRANT NUMBER(s): DNA 001-77-C-0220
9. PERFORMING ORGANIZATION NAME AND ADDRESS: SRI International, 333 Ravenswood Avenue, Menlo Park, California 94025	10. PROGRAM ELEMENT, PROJECT, TASK AREA & WORK UNIT NUMBERS: Subtask I25AAXHX633-40
11. CONTROLLING OFFICE NAME AND ADDRESS: Director, Defense Nuclear Agency, Washington, D.C. 20305	12. REPORT DATE: 1 October 1979 / 13. NUMBER OF PAGES: 52
14. MONITORING AGENCY NAME & ADDRESS (if different from Controlling Office)	15. SECURITY CLASS (of this report): UNCLASSIFIED / 15a. DECLASSIFICATION DOWNGRADING SCHEDULE

16. DISTRIBUTION STATEMENT (of this Report)

Approved for public release; distribution unlimited.

17. DISTRIBUTION STATEMENT (of the abstract entered in Block 20, if different from Report)

18. SUPPLEMENTARY NOTES

This work sponsored by the Defense Nuclear Agency under RDT&E RMSS Code B322078462 I25AAXHX63340 H2590D.

19. KEY WORDS (Continue on reverse side if necessary and identify by block number)

Auroral Zone Irregularities
Scintillation

20. ABSTRACT (Continue on reverse side if necessary and identify by block number)

This report describes the auroral-zone scintillation morphology as deduced from two years of observations made at Poker Flat, Alaska, using the DNA Wideband satellite. The data confirm that magnetic activity is the principal factor in determining the level of both nighttime and daytime auroral-zone scintillation. No systematic seasonal variation in activity was found, although the second year (1977-1978) showed a significant increase in overall activity when compared with the first year (1976-1977). This increase is

DD FORM 1 JAN 73 1473 EDITION OF 1 NOV 65 IS OBSOLETE

UNCLASSIFIED

SECURITY CLASSIFICATION OF THIS PAGE (When Data Entered)

20. ABSTRACT (Continued)

correlated with the general increase in solar activity, with the approach of the expected solar cycle maximum around 1980.

The average latitudinal distribution of the nighttime scintillation activity shows a pronounced enhancement at the point where the propagation path intercepts the local L shell. The scintillation enhancement is more prominent in the phase scintillation data; this has been attributed primarily to a geometrical effect, although there is evidence of a columnar F-region source that has contributed as well.

The latitudinal scintillation data have been sorted by magnetic activity. There is a general monotonic increase in scintillation activity as one proceeds poleward from the region of the diffuse aurora. Both the occurrence and severity of the scintillation data increases with increasing local magnetic activity. The daytime data, however, show a more definitive latitudinal boundary motion than do the nighttime data. Comparisons of premidnight and postmidnight data show the premidnight activity to be somewhat more intense.

PREFACE

The efforts of H. Jacobs, C. Code, G. Roach, R. Panton, J. Sheldon, R. Schledewitz, R. Evans, S. Evitt, and D. Lee, who operated and maintained the Poker Flat station during the two years of near continuous operations, are gratefully acknowledged.

CONTENTS

ILLUSTRATIONS

I INTRODUCTION AND SUMMARY

The high-latitude ionospheric irregularity structure that manifests itself in a variety of scintillation effects has been studied for many years. To define an equatorward boundary for the high-latitude scintillation region, Aarons et al. (1969) used the point where the amplitude scintillation index SI, measured at 54 MHz, first exceeds 50%. The global trace of this point is referred to as the high-latitude scintillation boundary. Poleward of the scintillation boundary, highly variable but generally enhanced radio-wave scintillation occurs.

Aarons (1973) has summarized the high-latitude scintillation morphology as deduced from a large and varied but consistently processed database. The scintillation boundary has an oval form about the geomatnetic pole, as does the auroral oval which identifies the average location of discrete auroral arcs. The scintillation boundary, however, is generally displaced several degrees equatorward of the auroral oval at night.

More recent observations have begun to show the detailed structure of the auroral-zone scintillation and its association with other auroral phenomena (Buchau et al., 1978; Martin and Aarons, 1977; Basu, 1975). In addition, the high-latitude irregularity structure has been sampled in situ (Sagalyn et al., 1974; Phelps and Sagalyn, 1976; Ahmed and Sagalyn, 1978). These analyses show that the high-latitude magnetospheric topology is consistent with the scintillation morphology in that the nighttime irregularity boundary, which has been associated with the equatorward edge of the soft central-plasma-sheet precipitation that causes the diffuse aurora, coincides with the scintillation boundary. Intense localized dayside scintillation has been associated with the cusp region. Localized nighttime scintillation enhancements within the scintillation boundary have been associated with active auroral arcs. This list, however, is by no means exhaustive; moreover, the work of identifying causal mechanisms has just begun.

In this report, we shall describe the morphology of the high-latitude scintillation observations made at Poker Flat, Alaska, using the Defense Nuclear Agency Wideband satellite. A detailed description of the experiment can be found in Fremouw et al., 1978. The satellite was launched on May 22, 1976, into a sun-synchronous polar orbit. Data were recorded at Poker Flat, Alaska, on a regular schedule for two years. After the two years of continuous operation, several intensive but comparatively short data-gathering campaigns were conducted.

The station at Poker Flat, Alaska is located at 65°7'N latitude, 140°3'W longitude, at a dip latitude of 65.4°N. During moderately disturbed auroral conditions, the midnight sector of the auroral oval passes over Poker Flat. The station is thus ideally located for measuring scintillation phenomena associated with the nighttime auroral oval.

The Wideband satellite orbit is such that southward-bound high-elevation passes occur at Poker Flat approximately at local midnight (1000 UT). Passes of progressively lower maximum-elevation angles occur before midnight to the east and after midnight to the west. The passes follow a trajectory nearly parallel to the geomagnetic meridian plane over Alaska. Figure 1 shows the 350-km ionospheric penetration paths for high-elevation day and night passes against an outline of the state of Alaska.

High-elevation daytime passes occur approximately nine hours after the corresponding nighttime passes because of the orbital inclination. They progress from the southeast to the northwest as shown in Figure 1. Because of the operating schedule, however, $\approx$ 30% fewer daytime passes than nighttime passes were recorded. The database is described in detail in Section II.

Before summarizing the principal results of the morphological study, it is useful to describe the detailed structure of a few representative individual passes. In Figure 2 we show a moderately disturbed evening pass recorded on 28 May 1976 (the first pass recorded). The scintillation indices are shown, plotted against Universal Time (UT). The Briggs-Parkin angle--the angle between the magnetic field direction and the

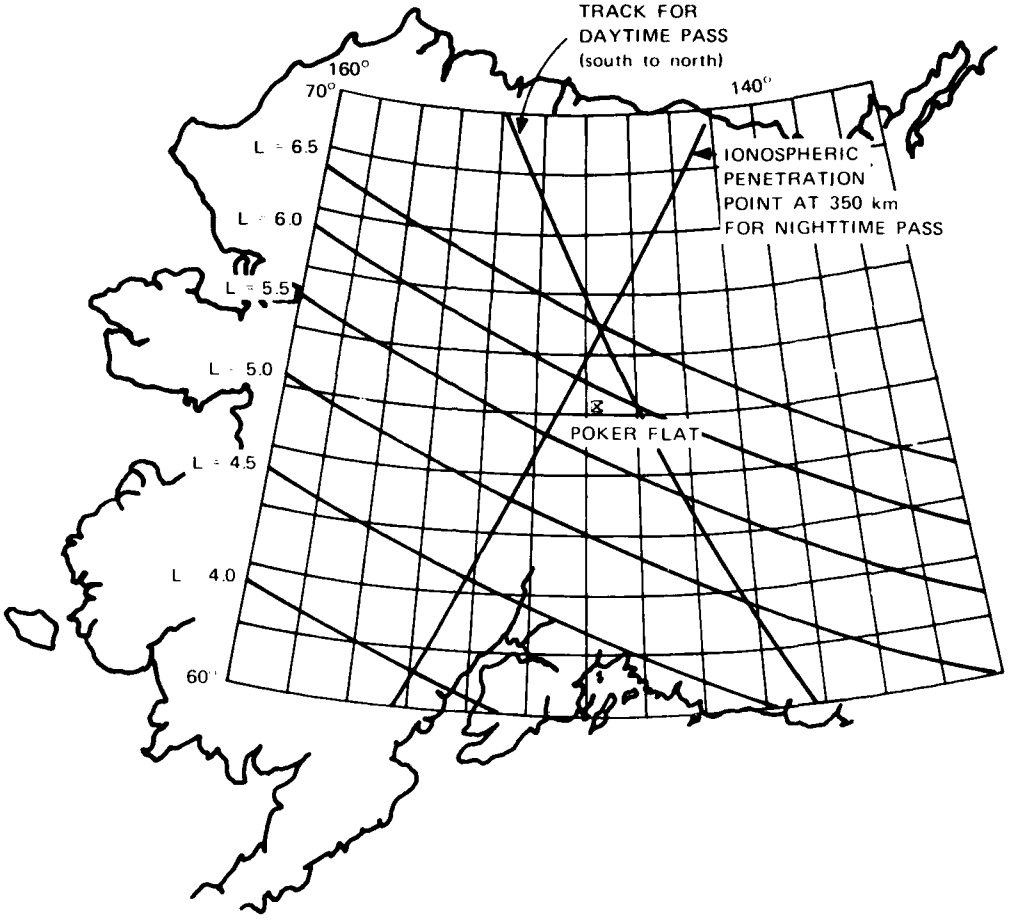

FIGURE 1 IONOSPHERIC PENETRATION POINT AT 350 km FOR TYPICAL HIGH-ELEVATION PASSES AT POKER FLAT

propagation vector--and the dip latitude at a 350-km reference altitude are also shown. The minimum Briggs-Parkin angle is marked on all of the displays. Because of the near meridional trajectory of the nighttime passes, this minimum occurs where the propagation vector lies within the L-shell. In the nighttime data, scintillation enhancements are almost certain to occur at this point.

A substorm onset--as indicated by an abrupt development of a negative bay on the College, Alaska, magnetometer--occurred during the pass. The phase-scintillation enhancement at 0954 UT is likely to be associated

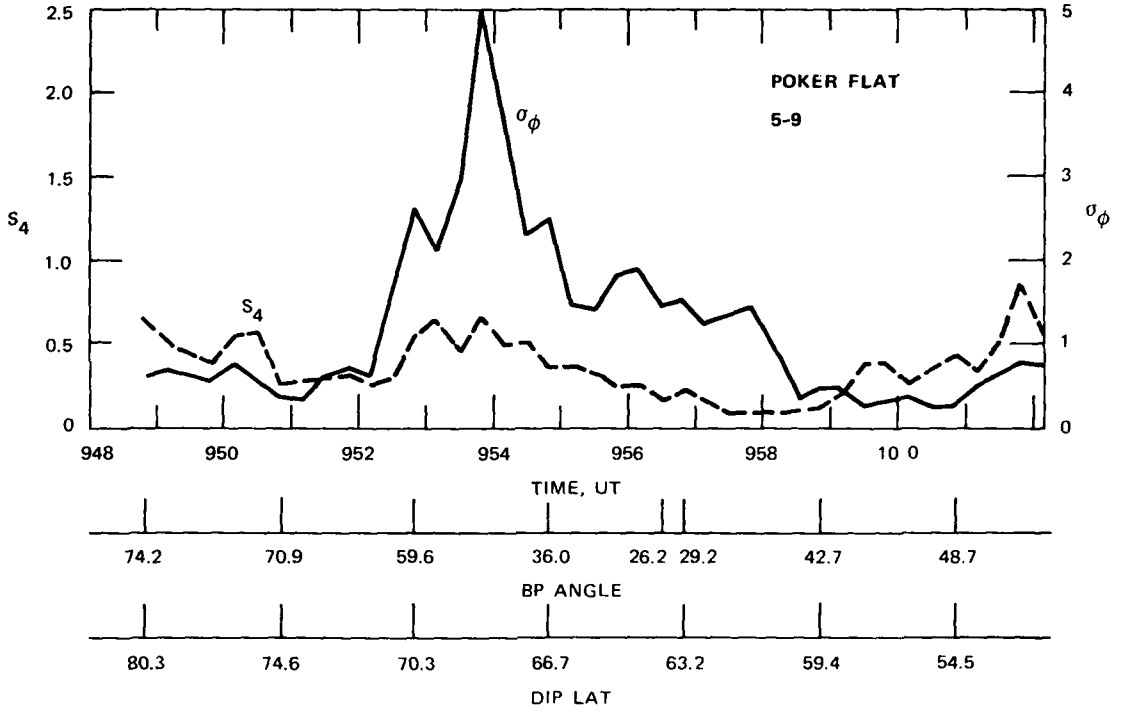

FIGURE 2 LATITUDINAL DISTRIBUTION OF AMPLITUDE AND PHASE SCINTILLATION FOR MODERATELY DISTURBED PASS

with the westward traveling surge generated by the substorm (local midnight at College occurs at 1000 UT). The region of enhanced phase scintillation between 0952 and 0955 is associated with a narrow region of enhanced energetic particle precipitation, as indicated by the corresponding total electron content data (not shown). The poleward scintillation boundary present in this particular pass, however, is not a common feature in the Poker Flat data.

A more typical pattern for moderately disturbed conditions is shown in Figure 3. Here an intense, localized, phase and amplitude scintillation enhancement is present well to the north of the station. The College magnetometer shows a positive bay, indicating that the substorm activity is well to the north of the station, although the poleward feature is most likely substorm related. In the center of the pass there is a broad region of enhanced phase scintillation.

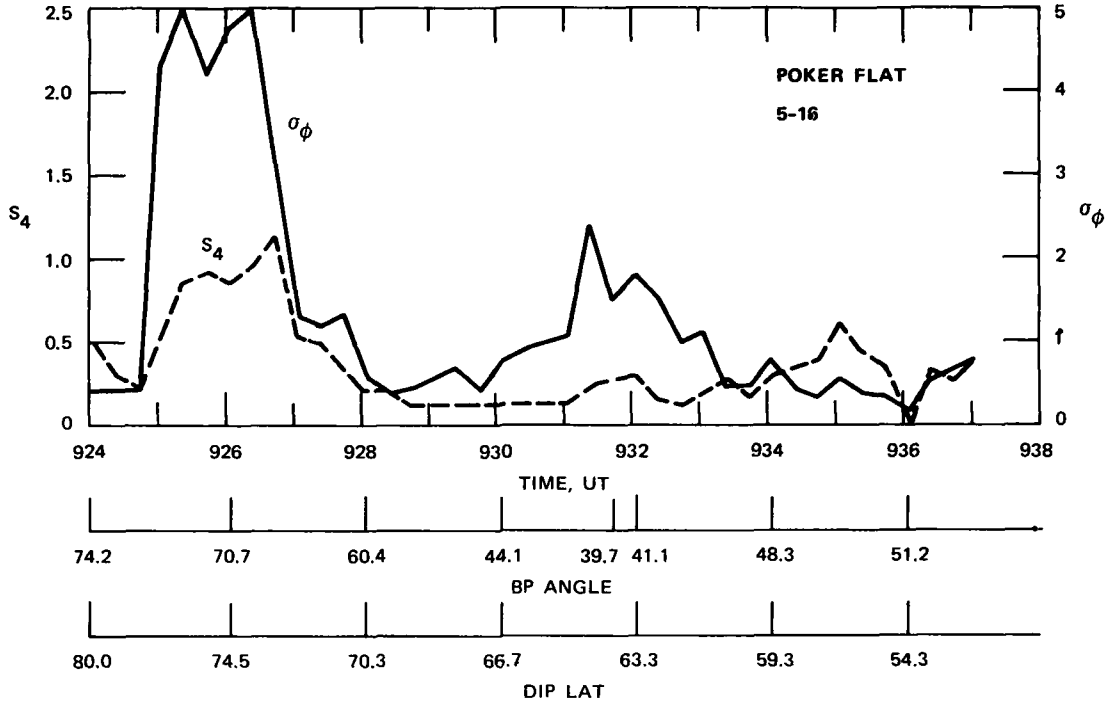

FIGURE 3 LATITUDINAL DISTRIBUTION OF AMPLITUDE AND PHASE SCINTILLATION SHOWING LOCALIZED PERTURBATION WELL TO THE NORTH OF POKER FLAT

In Figure 4, we show the typical pattern for sustained low-to-moderately-active conditions, when the substorm activity remains well to the north of the station. We believe that the narrow enhancement at the beginning of the pass is associated with the substorm activity. The most conspicuous feature, however, is a narrow phase-and-amplitude scintillation enhancement just at the point where the Briggs-Parkin angle minimizes. This feature has been attributed to a geometrical enhancement caused by sheet-like irregularity structures (Rino et al., 1978). The prominence of this scintillation feature was noted early in the Wideband data analysis (Fremouw et al., 1978).

The nighttime data show a general two-component structure. One component consists of narrow, highly variable scintillation enhancements that are almost certainly associated with active discrete aurora. A broader, more stable equatorward region of enhanced scintillation is associated with the diffuse aurora. Within the diffuse aurora there is

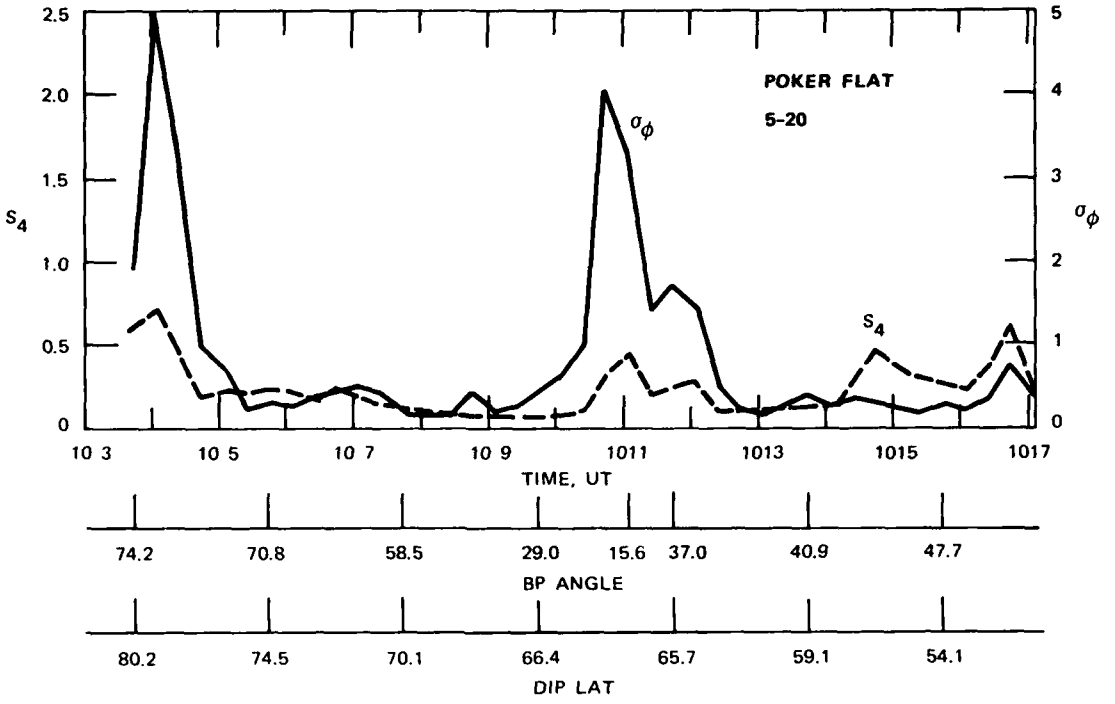

FIGURE 4 TYPICAL LATITUDINAL DISTRIBUTION OF AMPLITUDE AND PHASE *SCINTILLATION SHOWING* LOCALIZED ENHANCEMENT WHERE THE LINE-OF-SIGHT LIES WITHIN AN L-SHELL

a localized amplitude and phase scintillation enhancement that occurs whenever the propagation path is coincident with an L-shell.

These findings are in agreement with the aircraft observations of Buchau et al. (1978), who had good supporting optical data. They identified five regions, namely: the trough (I), diffuse aurora (III), and polar cap (V), with regions II and IV corresponding to the equatorward and poleward boundaries of the diffuse aurora, respectively.

The geometrical enhancement is most pronounced when it occurs near the edge of the diffuse aurora where a source region has been identified (Rino et al., 1978). This is evidently the Region-II enhancement observed by Buchau et al. (1978). The poleward boundary (Region IV) is where active arcs are most likely to occur. It should be noted that quiet auroral arcs produce enhanced phase scintillation but very little amplitude

scintillation (Buchau et al., 1978). The Poker Flat station is generally too far south for polar cap observations.

Daytime (morning) scintillation generally shows much broader regions of enhanced scintillation than do nighttime passes. Indeed, the most intense sustained-scintillation conditions occur during the daytime. An example is shown in Figure 5. There is no evidence of sheet-like structures in the daytime data, although localized (but randomly located) enhancements do occur.

The results that follow are based on the first two years of Wideband data collected at Poker Flat. The database and general data processing are described in Section II. In Section III we examine the general occurrence of activity. Scintillation is not at all uniformly distributed in the auroral zone. It was more frequent during the second year, in a period of increasing solar activity. Also, while there were months that were much more active than others, there is no evidence of seasonal control. By comparing general trends in scintillation activity and magnetic activity, we will see that, although the relationship is not simple, there is a good correlation between the two. This holds true for both night and daytime scintillation, which are quite different in nature.

Synoptic variations in scintillation are discussed in Section IV. The latitudinal distribution of activity shows that the most distinct feature in all of the auroral Wideband data is a pronounced enhancement of scintillation near the L shell, which is attributed to the formation at night of sheet-like irregularities. In some of the nighttime data, there is also evidence for an anomalous enhancement of activity far to the south. The latitudinal distribution of night and daytime activity is very different. A comparison of pre- and post-midnight passes shows, however, only minor differences. The latitudinal distribution of scintillation activity, when organized by magnetic activity level, shows good agreement between the occurrence of scintillation and the level of magnetic disturbance.

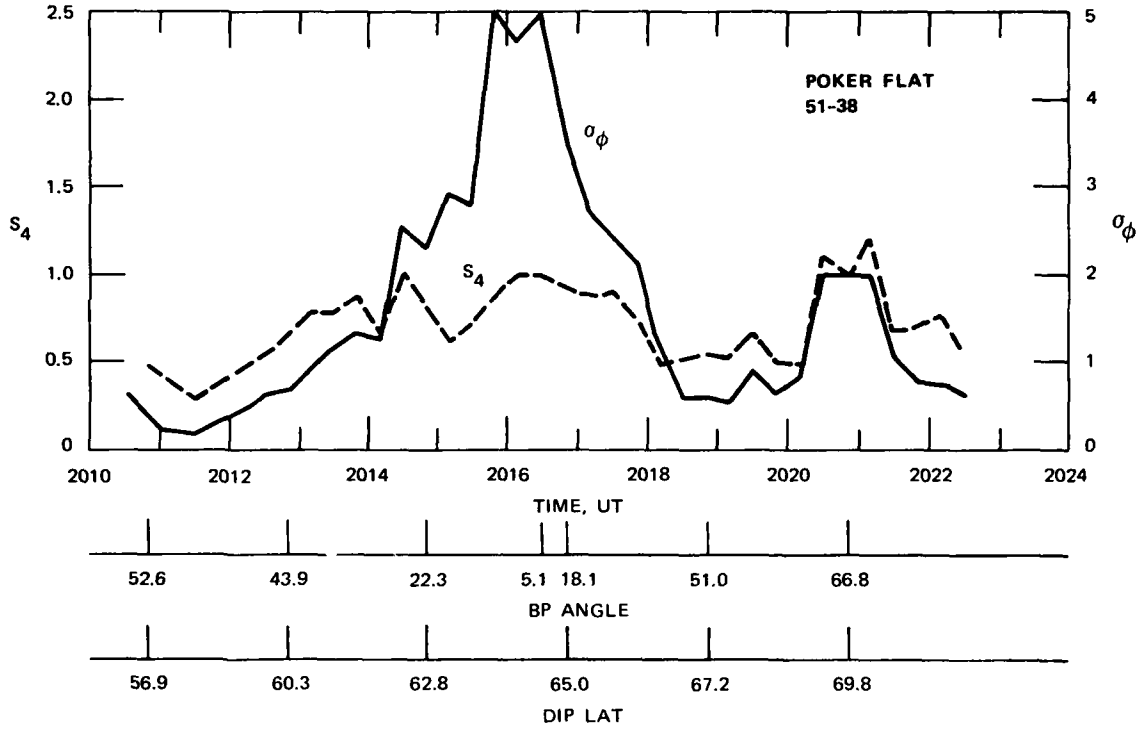

FIGURE 5 LATITUDINAL DISTRIBUTION OF AMPLITUDE AND PHASE SCINTILLATION FOR DISTURBED DAYTIME PASS

Finally, in Section V, we compare the Wideband data with the predictions for intensity scintillation at a given level of turbulence by the phase-screen model of scintillation, in order to isolate the purely geometrical factors.

II DATABASE

Routine data processing includes, as a first step, filtering out deterministic changes in the received signal, mainly power variations caused by changing range and slow-phase trends. A 0.1-Hz cutoff frequency is first used to remove the trend-like variations in the data. The scintillation data are then characterized by moments computed over 20-s intervals. These include the measured rms phase, σ_ϕ, and the intensity scintillation index, S_4, where $S_4 = (\langle I^2 \rangle - \langle I \rangle^2)^{1/2} / \langle I \rangle$ and I is the signal intensity. The S_4 index ranges from zero, for an undisturbed signal, to an upper limit near unity under conditions of strong scattering. System and sky noise place an effective lower limit on S_4 of about 0.02. The rms phase varies from a noise-controlled lower limit of about 0.1 rad to a virtually unlimited upper bound. The measured value of the rms phase is, however, controlled by the detrend filter cutoff, and no significance should be attached to its absolute value.

During the first two years of the experiment, the operating schedule called for recording nighttime passes three times per week and daytime passes once per week. As the Poker Flat station was the first remote field site in operation, and is also unique in some other aspects, it initially suffered a variety of equipment problems. Some of these problems continued to degrade certain types of data for several months. As a result, there exist some gaps in the data for the first year, and careful editing was necessary, with an eye toward retaining as large a sample as possible. The net result, however, is an excellent database covering the time from May 1976 until April 1978. In 1976-1977, a total of 284 complete or partial passes were retained, and 449 passes were collected in 1977-1978. Changes in data-collection technique make for some differences in the database over time, for example in the latitudinal coverage, and these will be pointed out.

Typically, two or three satellite passes would be recorded during each of the scheduled night and day operating times. Sometimes, more intensive data-taking was scheduled for coordinated experiments near the equinoxes. Passes of less than 30° maximum elevation were routinely ignored, and generally the first and last 10° of elevation were masked out to avoid multipath effects.

III OVERALL S_4 AND σ_ϕ STATISTICS

Figures 6 and 7 give a broad overview of the first two years of the Wideband experiment. The passes were grouped into two bins per month, in order to provide valid statistical samples, without obscuring short-term variations. Figure 6 displays the data taken between May 1976 and April 1977; Figure 7 is for the same period in 1977-1978. Each figure gives separately a graph of S_4 exceedence statistics, σ_ϕ exceedence statistics, and an average of the three-hour K magnetic index as recorded at nearby College, Alaska.

Exceedence statistics are derived as follows: Five levels of S_4 and σ_ϕ have been selected; S_4 = 0.2, 0.4, 0.6, 0.8, and 1.0, and σ_ϕ = 1, 2, 3, 4, and 5. The ordinate which is labeled Percent Occurrence indicates the percentage of the observation time that the ordinate value was exceeded. For instance, in the first half of June 1976, the 0.2 value of S_4 was exceeded about 35% of the time, the 0.4 value about 9% of the time, and the σ_ϕ value of 1 was found to be exceeded about 20% of the observation time. The numbers at the top of each bin indicate the numbers of passes and the number of 20-s data samples that form that particular measurement.

Between the plots marked Average College K and the σ_ϕ histograms, the number of passes contained in each bin and the total number of 20-s data points are indicated. For the sake of completeness, all of the edited data has been displayed, and so care should be taken in interpreting the activity of bins containing relatively little data. For example, only two passes were saved from the first half of October 1976, but the bin has the highest percent occurrence levels of scintillation for the first year.

The graphs at the tops of Figures 6 and 7 give some indication of the magnetic activity for these years. The three-hour College K magnetic

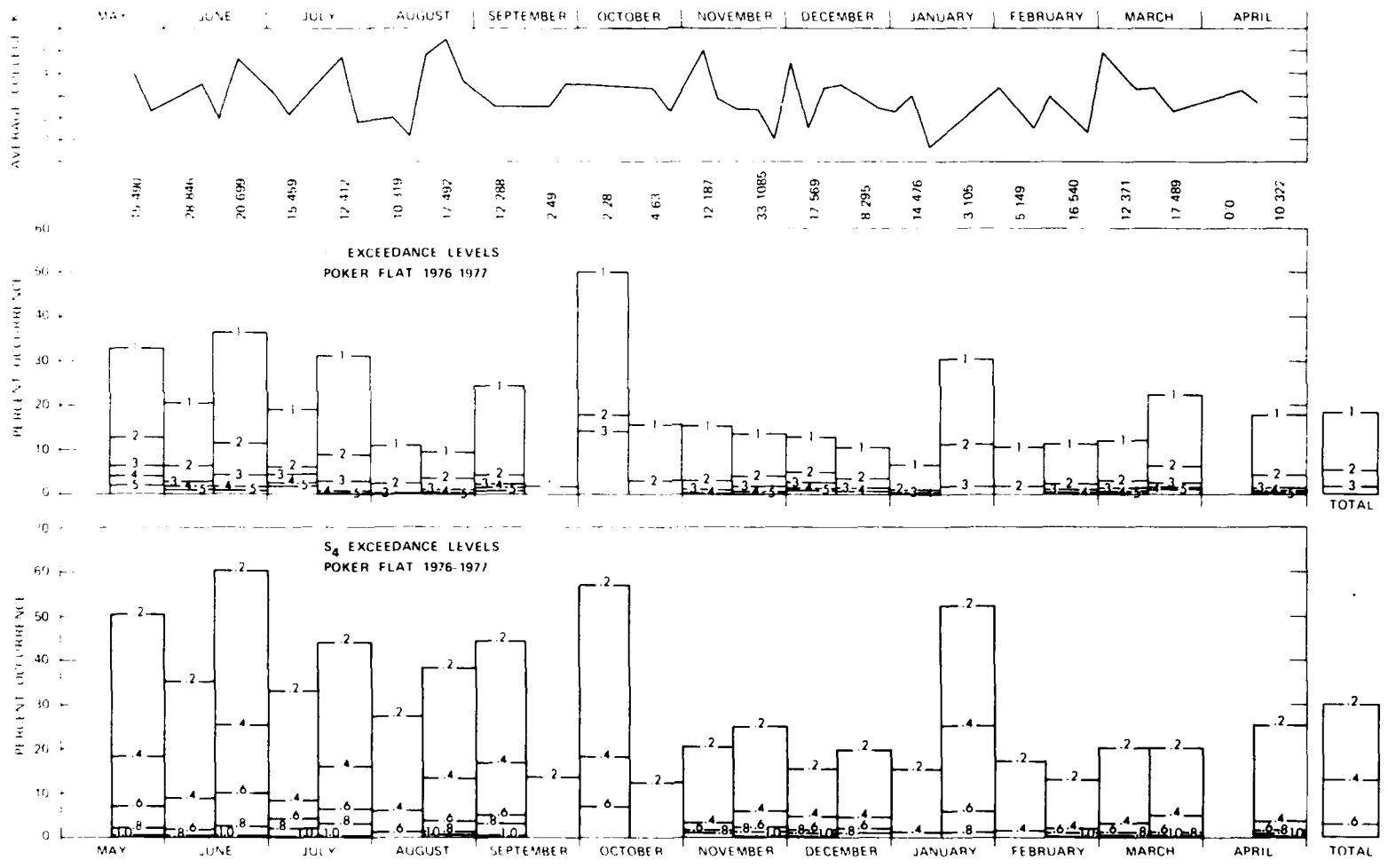

FIGURE 6 AMPLITUDE AND PHASE SCINTILLATION EXCEEDANCE STATISTICS FOR 1976-1977 DATA

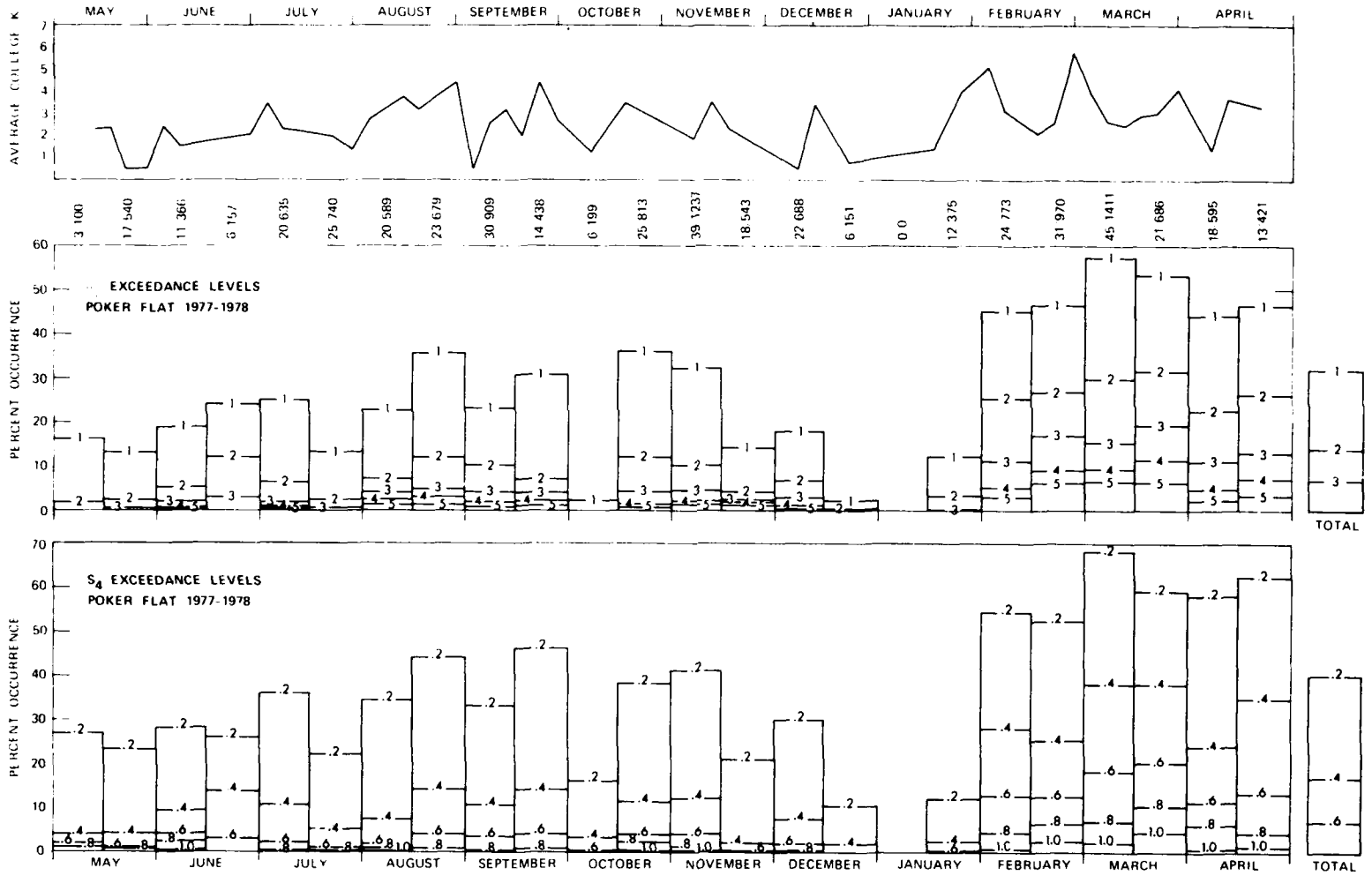

FIGURE 7 AMPLITUDE AND PHASE SCINTILLATION EXCEEDANCE STATISTICS FOR 1977-1978 DATA

index was recorded for each pass, and these values were averaged weekly. No striking patterns of activity are obvious in these displays, but there are more subtle patterns evident. The activity does not follow a point-by-point correlation with the magnetic disturbance, for instance, but there is overall agreement. As an example, in the summer months of 1976, scintillation occurred with greater frequency in the later half of each month, and this matches peaks in magnetic activity very well. During the winter months, however, there are two sharp peaks in the average College K index for which there is no attendant rise in scintillation. Nonetheless, the overall trend in magnetic activity during this period is downward, which matches the decline in frequency of scintillation.

Although a peak in the average local magnetic activity is most often associated with an enhancement of scintillation, the intensity of the magnetic disturbance need not cause a proportionate increase in the scintillation activity. Again, in the summer months of 1976, the greatest magnetic activity occurred during satellite passes recorded in late August. There is an increase in the scintillation activity during this period, but it is lower than previous peaks in June and July when magnetic disturbances were lower. Similar patterns are evident in the 1977-1978 data summarized in Figure 7.

It is apparent from these figures that phase and amplitude scintillation track very well in this type of averaging. It is, therefore only necessary, when comparing different data populations, to use either one or the other. In Figures 8 and 9 the σ_3 values for night and daytime passes for each year are compared. It is clear that the second year was much more active than the first. This is seen clearly in the total exceedance levels for each year. For night passes (Figure 8) in 1976-1977, the 1-radian level was exceeded only 21% of the time, while the same level eas exceeded 39% in 1977-1978. Scintillation was not only more frequent but also more intense; as an example, the 5-radian level of σ_3 was exceeded more the second year than was the 3-radian level during the first year.

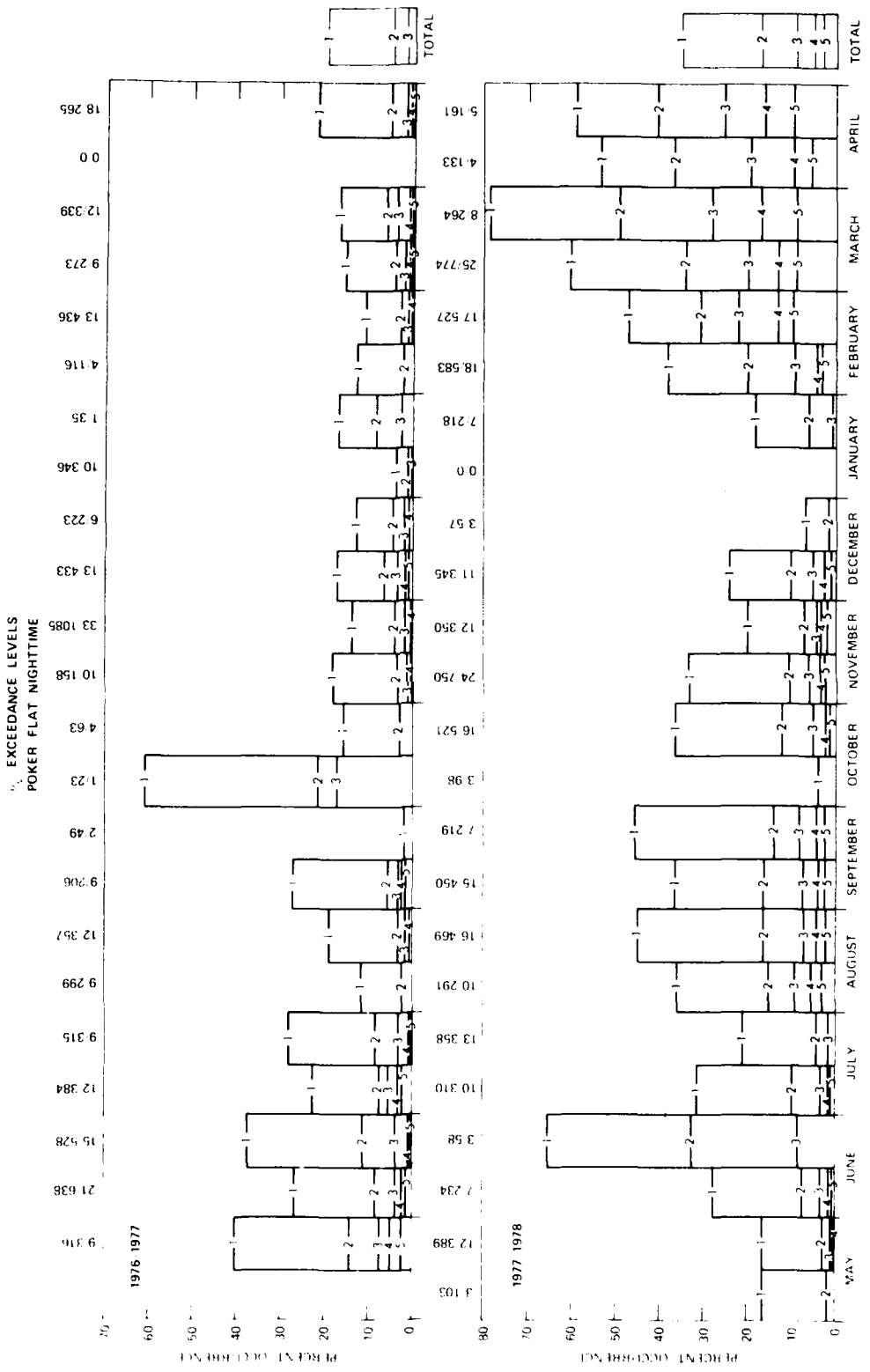

FIGURE 8 PHASE EXCEEDANCE LEVELS FOR NIGHTTIME DATA ONLY

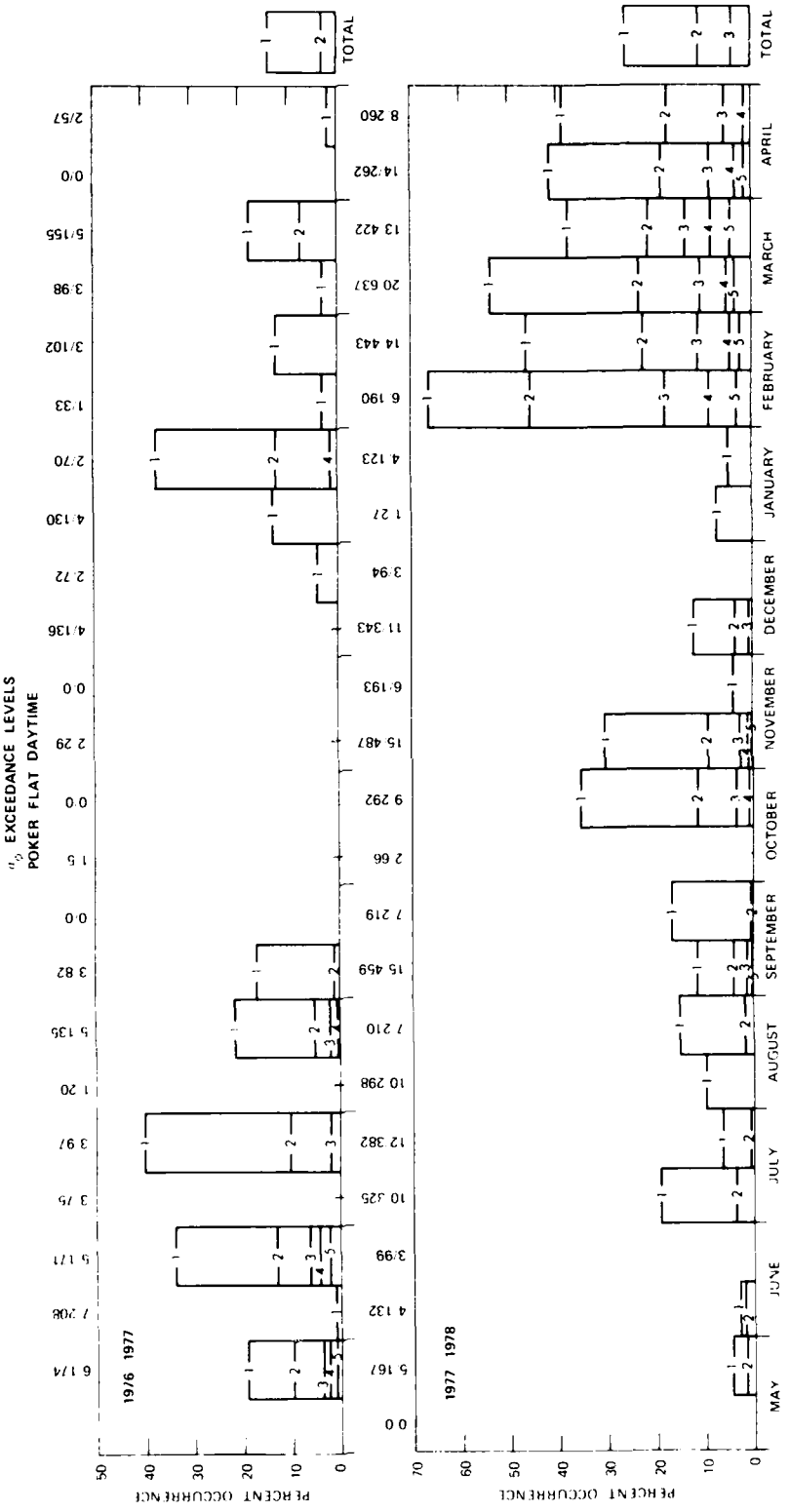

FIGURE 9 PHASE EXCEEDANCE LEVELS FOR DAYTIME DATA ONLY

There is no pronounced seasonal variation in the exceedence statistics. The scintillation during 1976-1977 is most frequent in a broad period around summer solstice. This is not the case in 1977-1978, when the most active periods occurred near the spring equinox. There is nothing in the winter of 1977 like the broad intense occurrence of scintillation in the winter of 1978.

The daytime exceedence levels are shown in Figure 9. As discussed in the introduction, daytime scintillation is evidently caused by different mechanisms than nighttime scintillation. The daytime scintillation of 1977-1978, however, is grouped in the same general periods as the night activity, and is evidently correlated in a similar fashion with magnetic disturbances. Unfortunately, the daytime results of 1976-1977 contain very few passes.

IV SPATIAL AND TEMPORAL MORPHOLOGY

A. Latitudinal Distribution

To examine the latitudinal structure of the auroral-zone scintillation, S_4 and σ_ϕ statistics were grouped into bins of magnetic dip latitude 2.5° wide. The level of activity, which was exceeded by half of the data points, was then determined for each bin. This method was used, rather than a simple average, in searching for scintillation sources, because the method minimizes contributions from a few very quiet or very disturbed passes.

Figures 10 and 11 show the latitudinal distribution of the nighttime phase and intensity scintillation respectively. The number of 20-s data points in each bin of the histogram is included beneath the curve. The increased activity during 1977-1978 is clearly evident in the phase data. The most striking result, however, is the region of enhanced activity near 64° dip latitude (L shell = 5.5). This enhancement is the most characteristic feature of the Wideband data. It is believed that the enhancement is a geometrical effect that occurs when the propagation vector aligns itself with irregularities which are highly elongated, not only along the local direction of the magnetic field but also in the plane of the local L-shell (Rino et al., 1978). The geometrical enhancement is more pronounced in phase scintillation (Figure 10) than it is in the scintillation intensity (Figure 11), which is in agreement with the weak scatter theory (Rino, 1979).

The distribution of activity in these figures is asymmetric about the zenith. The strength and frequency of scintillation both grow steadily to the north of the station. Behavior to the south is generally more quiet, except for an anomalous increase in activity at the very southern limits of the data in the first year, particularly in the intensity scintillation (Figure 11). The second year does not show such

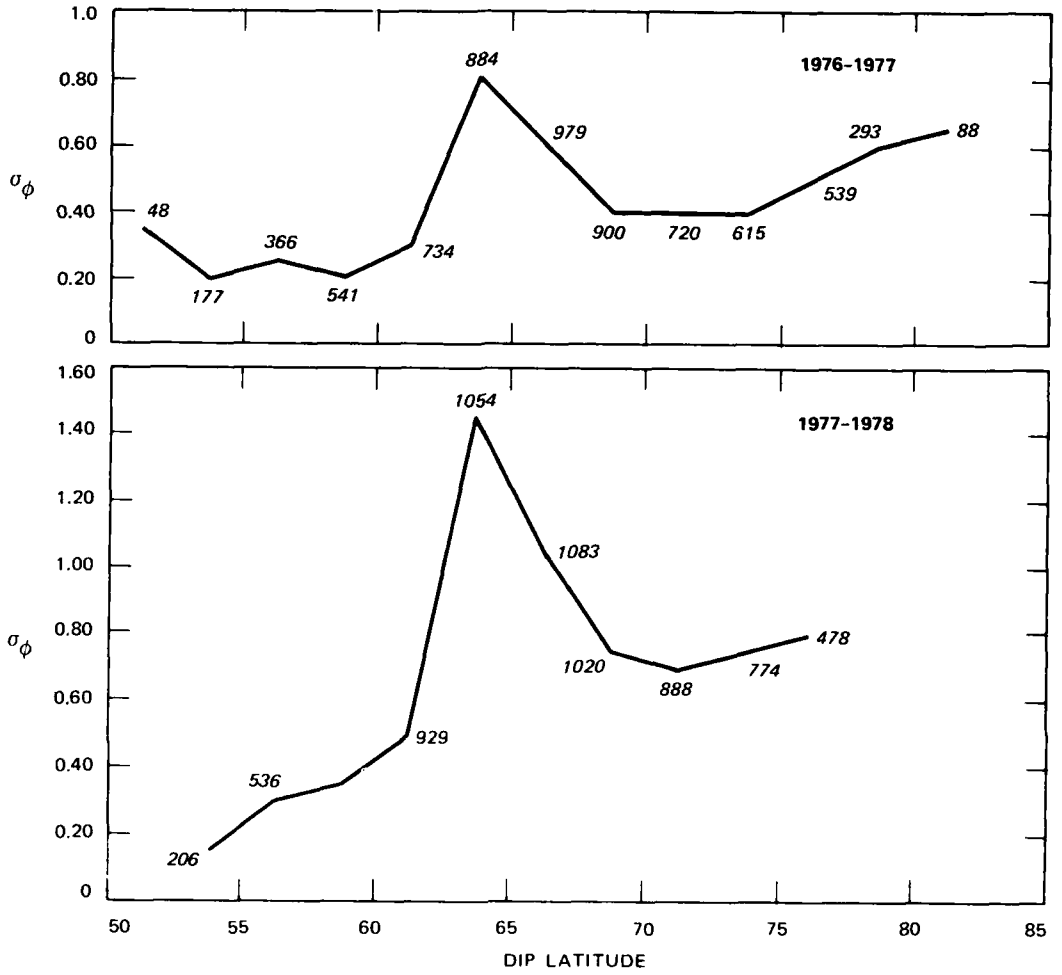

FIGURE 10 RMS PHASE AT 50% EXCEEDANCE LEVEL vs. MAGNETIC LATITUDE FOR NIGHTTIME DATA

an increase, but the latitudinal extent of this data is less than in the first year. The difference in latitudinal coverage of the data between the two years resulted from a change in the elevation limits for each pass, and also from a change in the detrending process which required a longer filter settling time.

The relatively few data points contributing to the southern enhancement, plus the fact that these data are almost all from the initial months of operation when ground effects were a recurring problem, make these

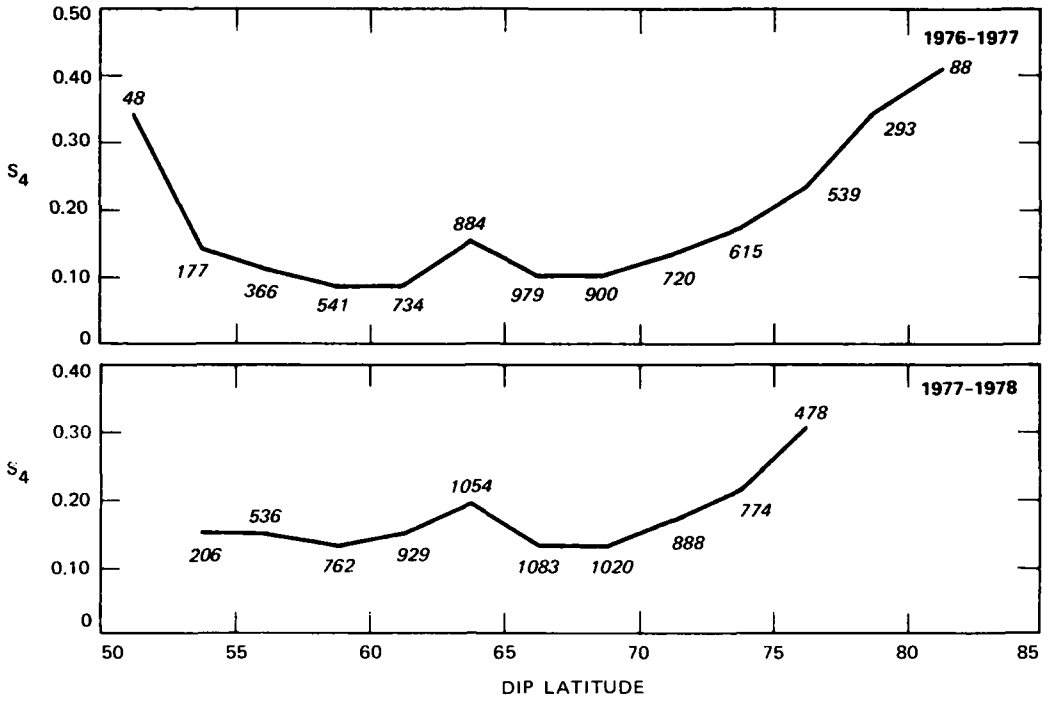

FIGURE 11 S_4 AT 50% EXCEEDANCE LEVEL vs. MAGNETIC LATITUDE FOR NIGHTTIME DATA

data somewhat suspect. Even though ground effects have been carefully edited from the database, they may occasionally be hidden in more moderate activity. It appears, nonetheless, that the source is genuine.

In striking contrast to the latitudinal distribution of the nighttime scintillarion is the smooth pattern of daytime activity (Figure 12). The strength and frequency of the intensity scintillation of the second year increases with dip latitude, and there is no evidence of the sheet-like irregularities. The sheet-like irregularities have been associated with the major nighttime particle-precipitation regions which are not present during the day.

B. Pre-Midnight and Post-Midnight Variations of Scintillation Activity

In Figures 13 and 14 the S_4 50%-exceedence levels of nighttime data are divided into passes occurring before and after midnight. For the

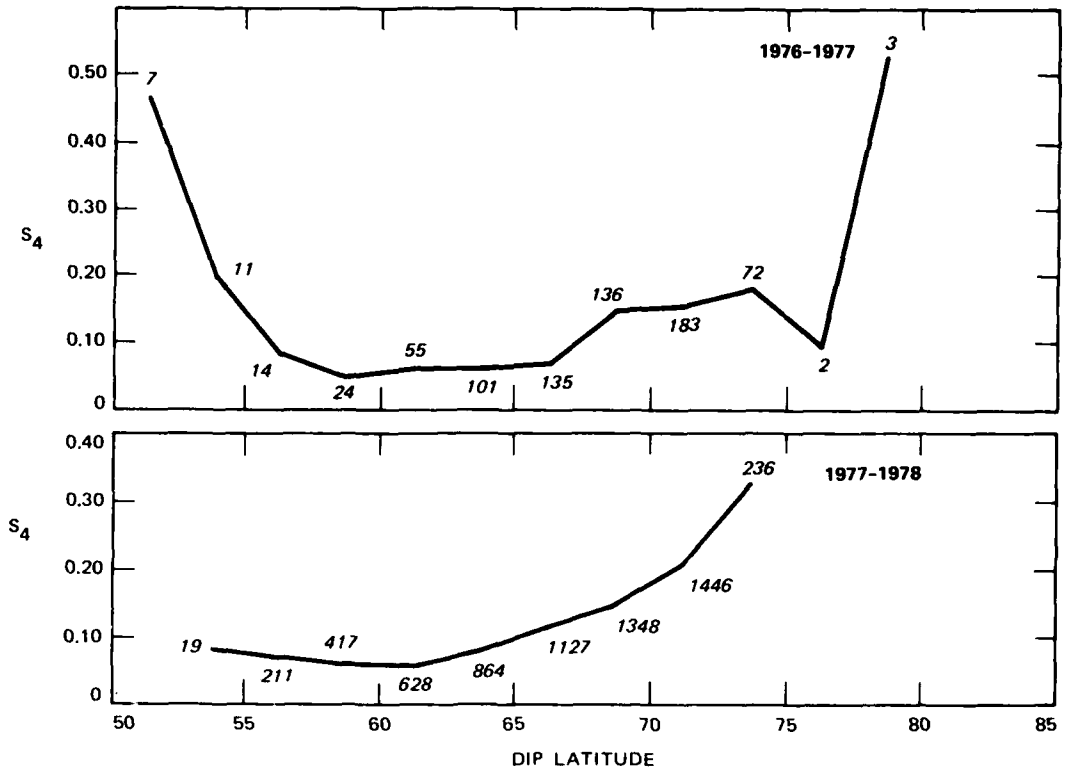

FIGURE 12 S_4 AT 50% EXCEEDANCE LEVEL vs. MAGNETIC LATITUDE FOR DAYTIME DATA

first year the pre-midnight data is somewhat higher than the post-midnight; moreover, the poleward enhancement is more gradual in the post-midnight data, suggesting that the auroral activity tends to be closer to the station and/or more evenly distributed. This type of activity would be expected, based on the differences in structure between the evening and the morning visual auroral patterns.

The pre-midnight data of the second year (Figure 14) show a widening of the region of the geometrical enhancement when compared with the 1976-1977 pattern of the post-midnight data. As conditions were generally more active during the second year, this behavior is indicative of more substorm activity near the station. The pattern of generally higher scintillation activity persists in the 1977-1978 data.

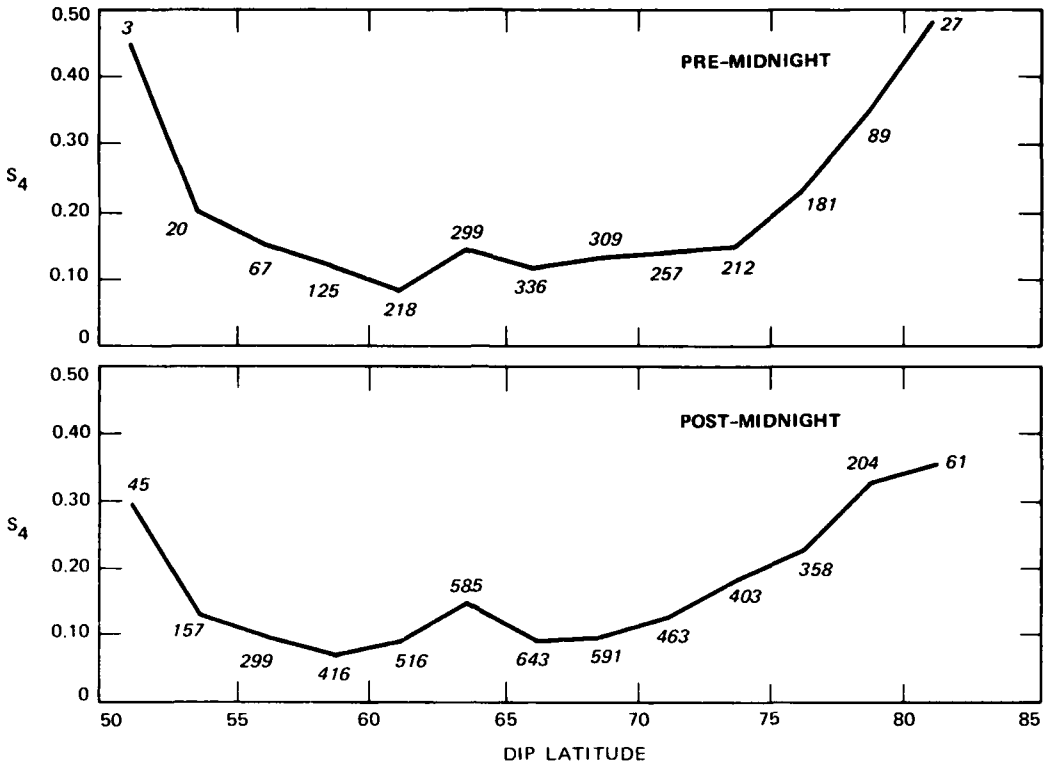

FIGURE 13 S_4 AT 50% EXCEEDANCE LEVEL vs. MAGNETIC LATITUDE FOR 1976-1977 NIGHTTIME DATA WITH PRE- AND POST-MIDNIGHT TIME SECTORS PLOTTED SEPARATELY

C. Seasonal Variation of Latitudinal Structure

The histograms of nighttime intensity scintillation for each year are divided into seasons centered around the solstices and equinoxes (Figures 15 and 16). In discussing the overall results in Section III, we found no correlation of activity with the seasons. This conclusion is verified by these figures. While activity varies considerably from one season to the next, there is no correlation between the same seasons of the two years. The period February through April, for example, was the most active time of the second year (Figure 16), while the same period was the most quiet time of the first year.

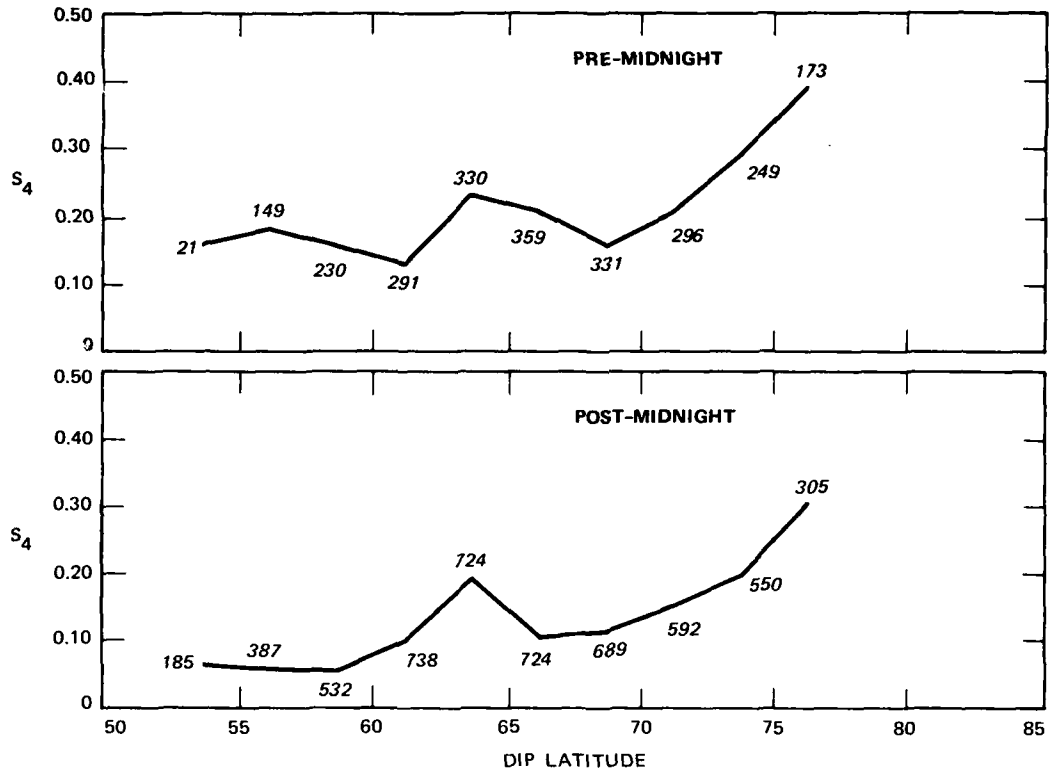

FIGURE 14 S_4 AT 50% EXCEEDANCE LEVEL vs. MAGNETIC LATITUDE FOR 1977-1978 NIGHTTIME DATA WITH PRE- AND POST-MIDNIGHT TIME SECTORS PLOTTED SEPARATELY

D. Scintillation and Magnetic-Activity Dependence of Latitudinal Structure

To explore the relationship of scintillation to magnetic activity, histograms of the occurrence frequency for S_4 exceeding 0.3, and σ_ϕ exceeding 1.0 radian (approximately the transition from weak-to-strong scatter regimes) were sorted according to the College three-hour K index. The local K index was used; it was generally a better reference for ordering the data than the planetary index.

The K values varied mostly from 0 to 7; the rare value greater than 7 was included in that grouping. Figures 17 and 18 display nighttime S_4 and σ_ϕ for the first year. The number of 20-s data points included in 5° of dip latitude is shown (bins are again 2.5° wide).

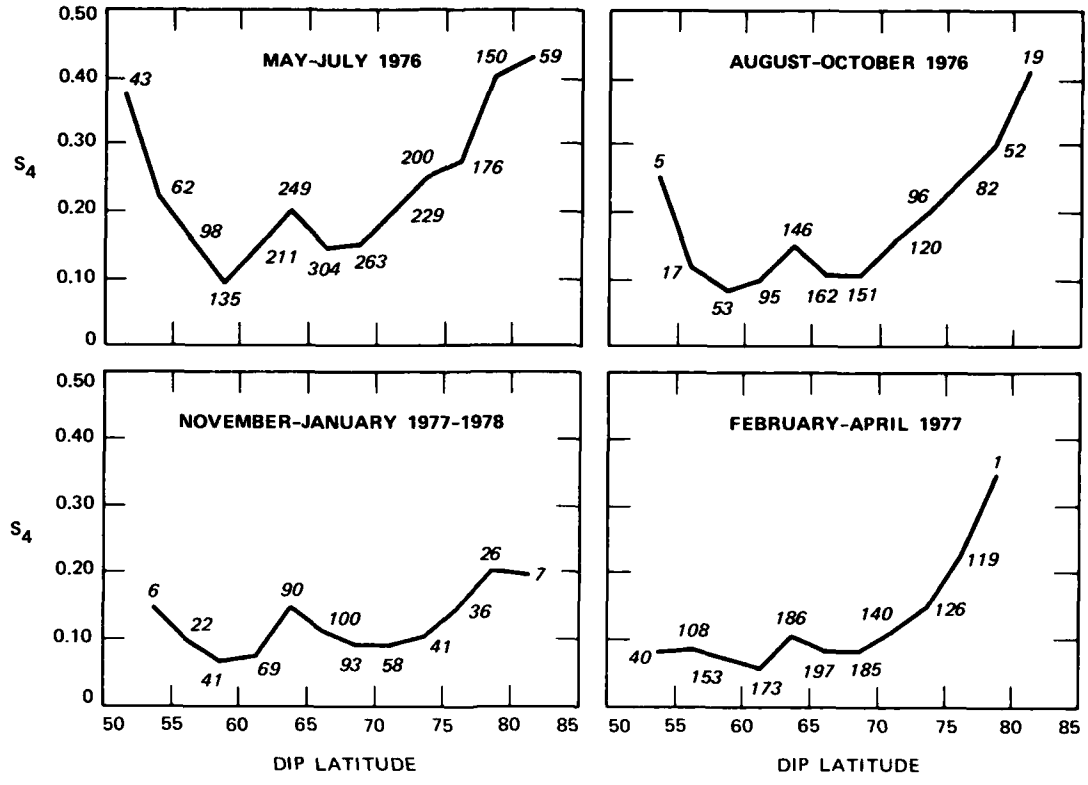

FIGURE 15 S_4 AT 50% EXCEEDANCE LEVEL vs. MAGNETIC LATITUDE FOR 1976-1977 NIGHTTIME DATA FOR CONSECUTIVE 3-MONTH PERIODS

The latitudinal distribution of the nighttime scintillation data shows evidence of both a general enhancement with increasing K as well as equatorward migration. This is more clearly evident in the 1977-1978 data shown in Figures 19 and 20 where the southern enhancement is not present. It should be noted that the southern enhancement is present in the 1976-1977 data during less active (K = 1,2) conditions, which supports the hypothesis that it is associated with the plasma pause.

The occurrence of strong daytime scintillation is more highly correlated with magnetic activity than in the nighttime data. This is seen in the histograms of Figures 21 and 22 (second-year results). The frequency of scintillation can be dramatic--e.g., when $K \geq 5$, σ_ϕ exceeds 1 radian almost 100% of the time in the active region (Figure 22). The daytime data also show more evidence of boundary motion with varying activity.

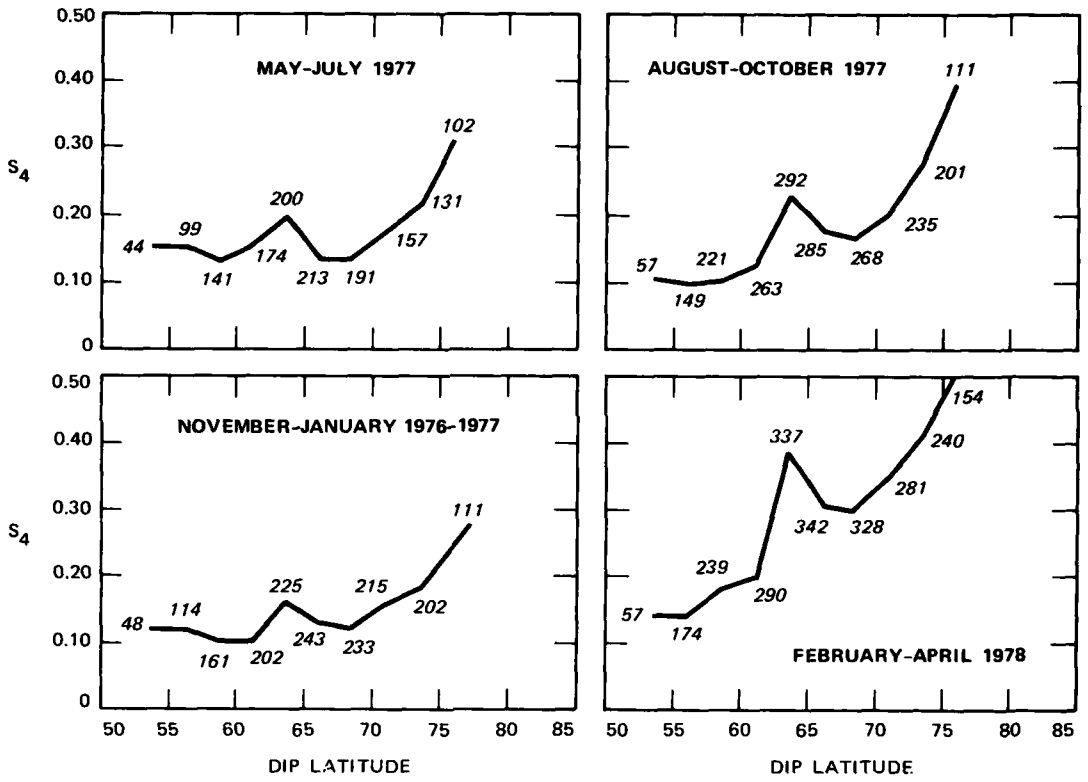

FIGURE 16 S_4 AT 50% EXCEEDANCE LEVEL vs. MAGNETIC LATITUDE FOR 1977-1978 NIGHTTIME DATA FOR CONSECUTIVE 3-MONTH PERIODS

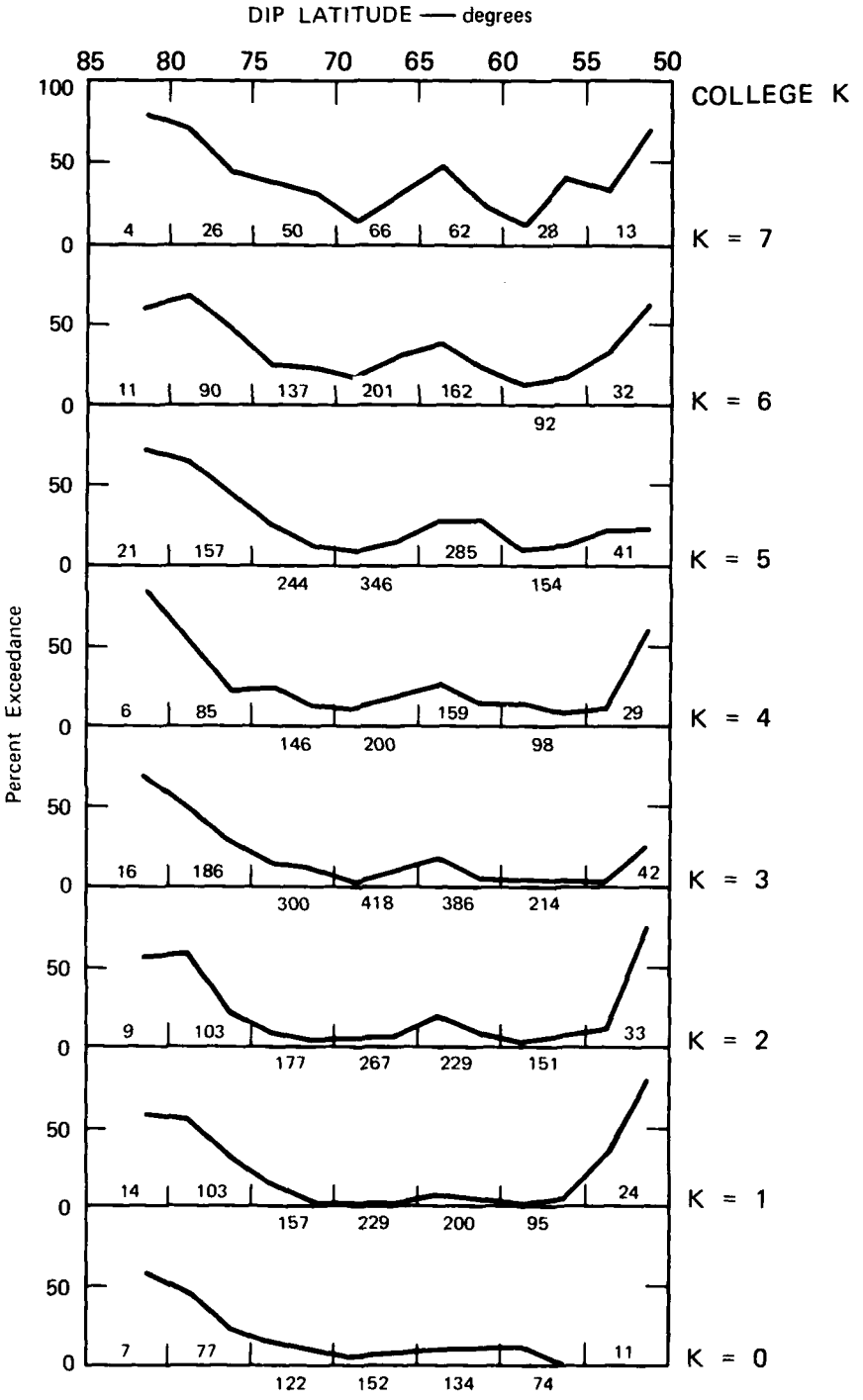

FIGURE 17 DEPENDENCE OF LATITUDINAL DISTRIBUTION S_4 = 0.3 EXCEEDANCE LEVEL ON LOCAL MAGNETIC ACTIVITY, 1976-1977 DATA

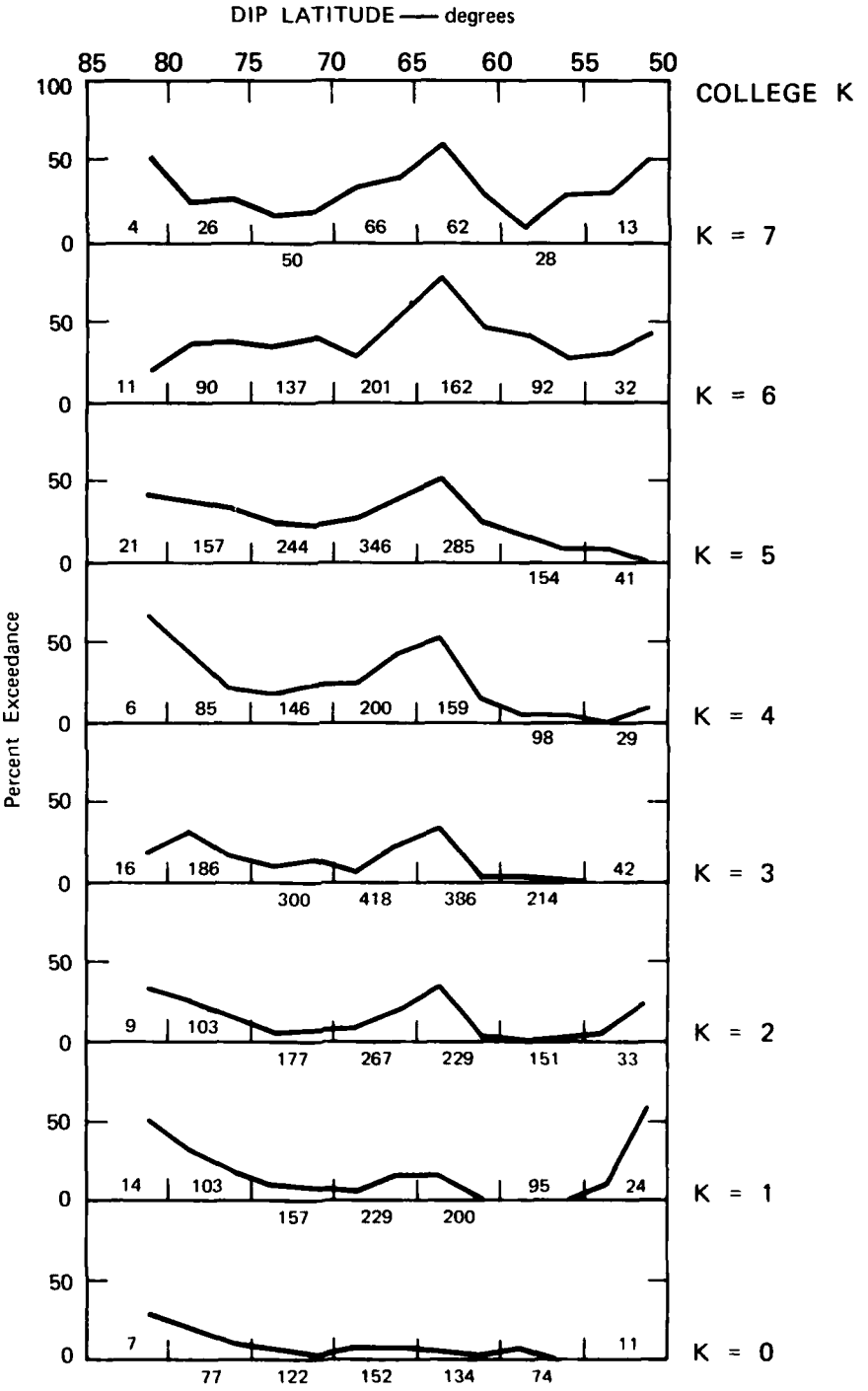

FIGURE 18 DEPENDENCE OF LATITUDINAL DISTRIBUTION OF NIGHTTIME σ_ϕ = 1 RADIAN EXCEEDANCE LEVEL ON LOCAL MAGNETIC ACTIVITY, 1976-1977 DATA

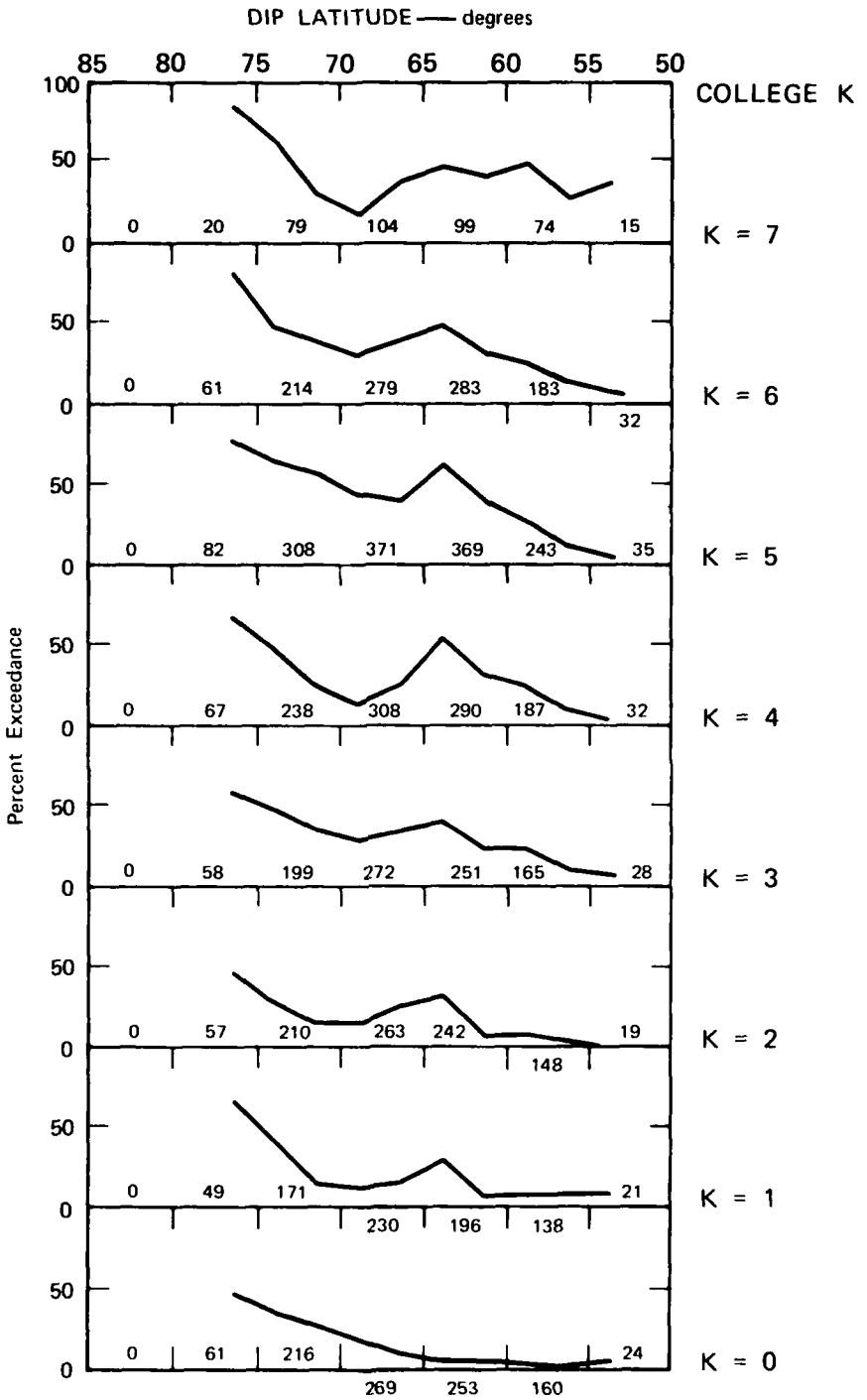

FIGURE 19 DEPENDENCE OF LATITUDINAL DISTRIBUTION OF NIGHTTIME S_4 = 0.3 EXCEEDANCE LEVEL ON LOCAL MAGNETIC ACTIVITY, 1977-1978 DATA

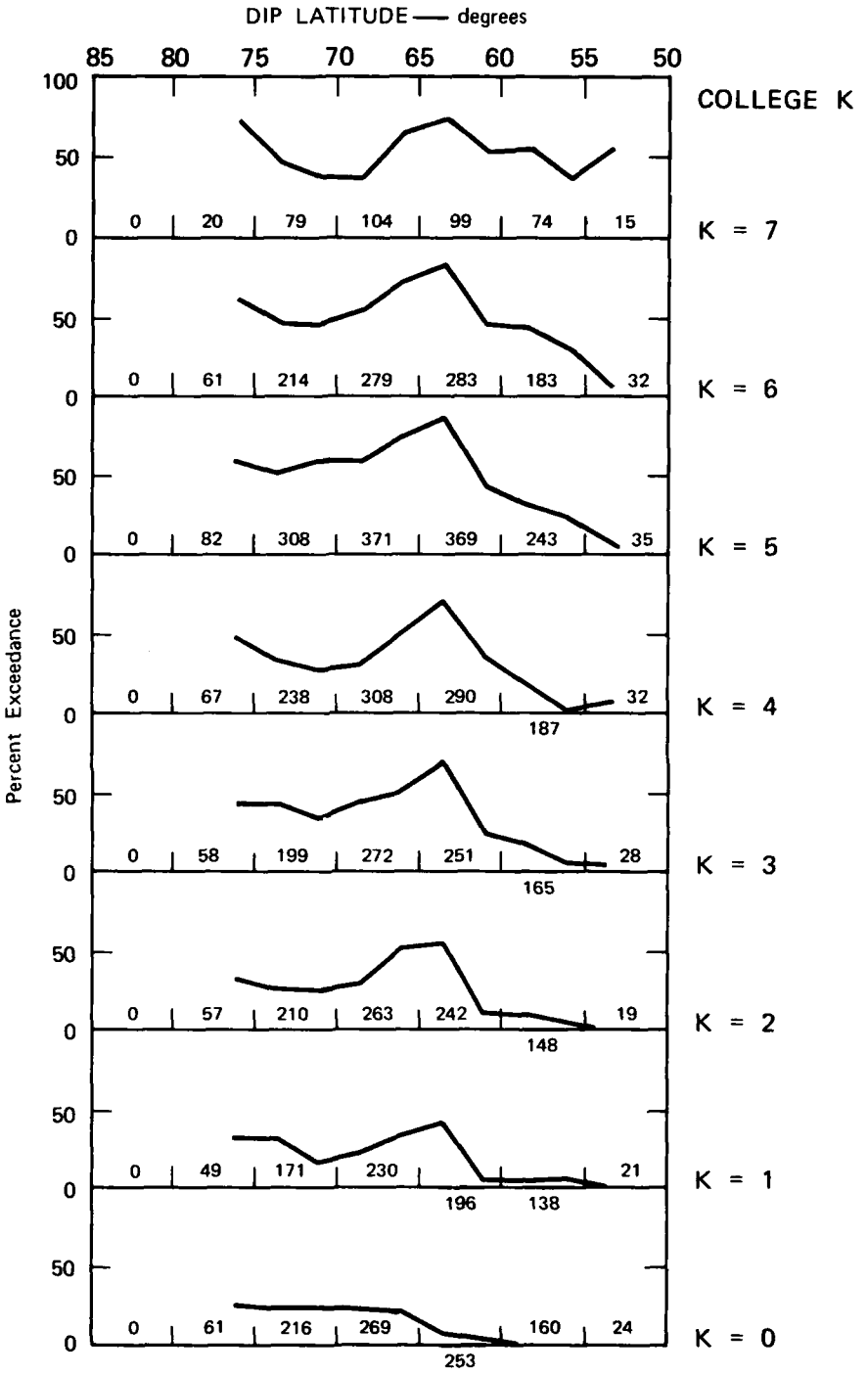

FIGURE 20 DEPENDENCE OF LATITUDINAL DISTRIBUTION OF NIGHTTIME σ_ϕ = 1 RADIAN EXCEEDANCE LEVEL ON LOCAL MAGNETIC ACTIVITY, 1977-1978 DATA

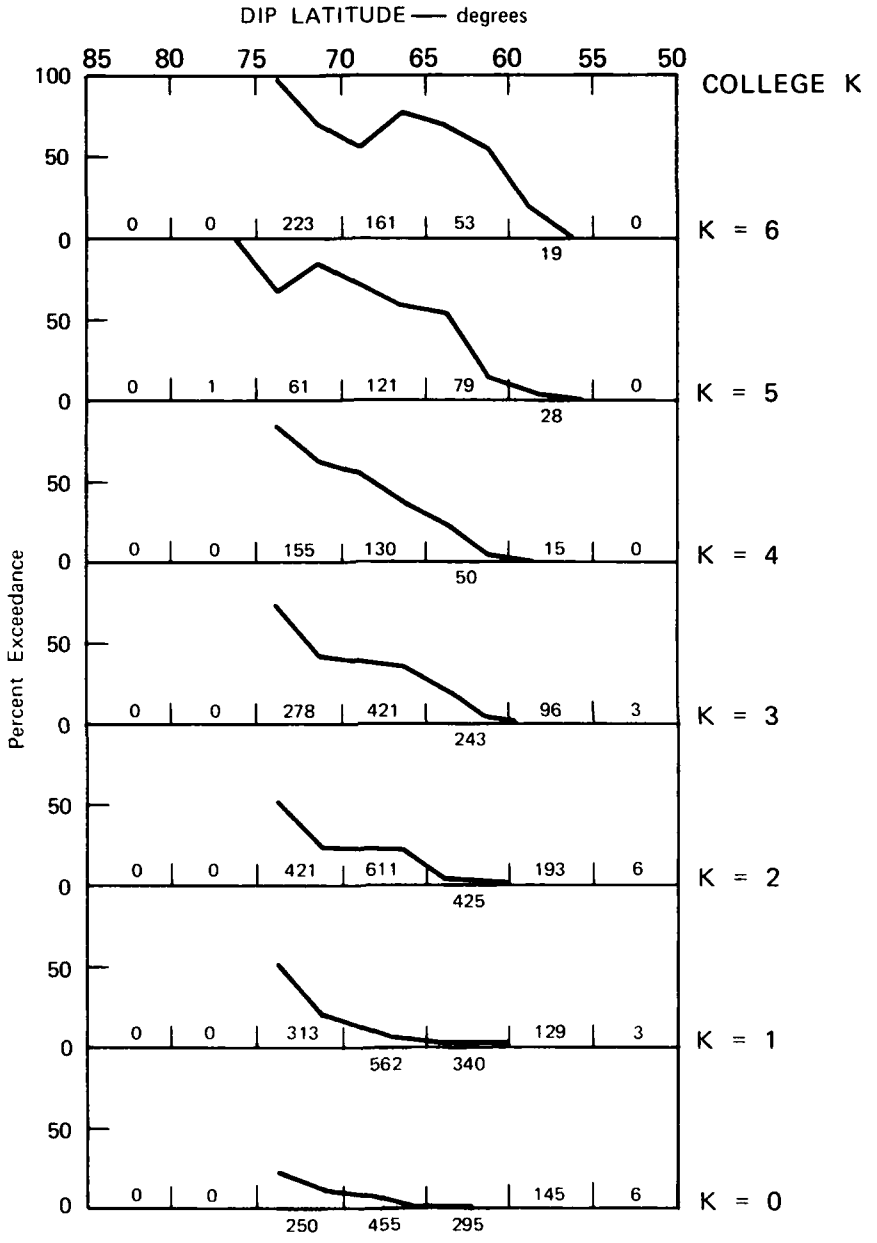

FIGURE 21 DEPENDENCE OF LATITUDINAL DISTRIBUTION OF DAYTIME S_4 = 0.3 EXCEEDANCE LEVEL ON LOCAL MAGNETIC ACTIVITY, 1977-1978 DATA

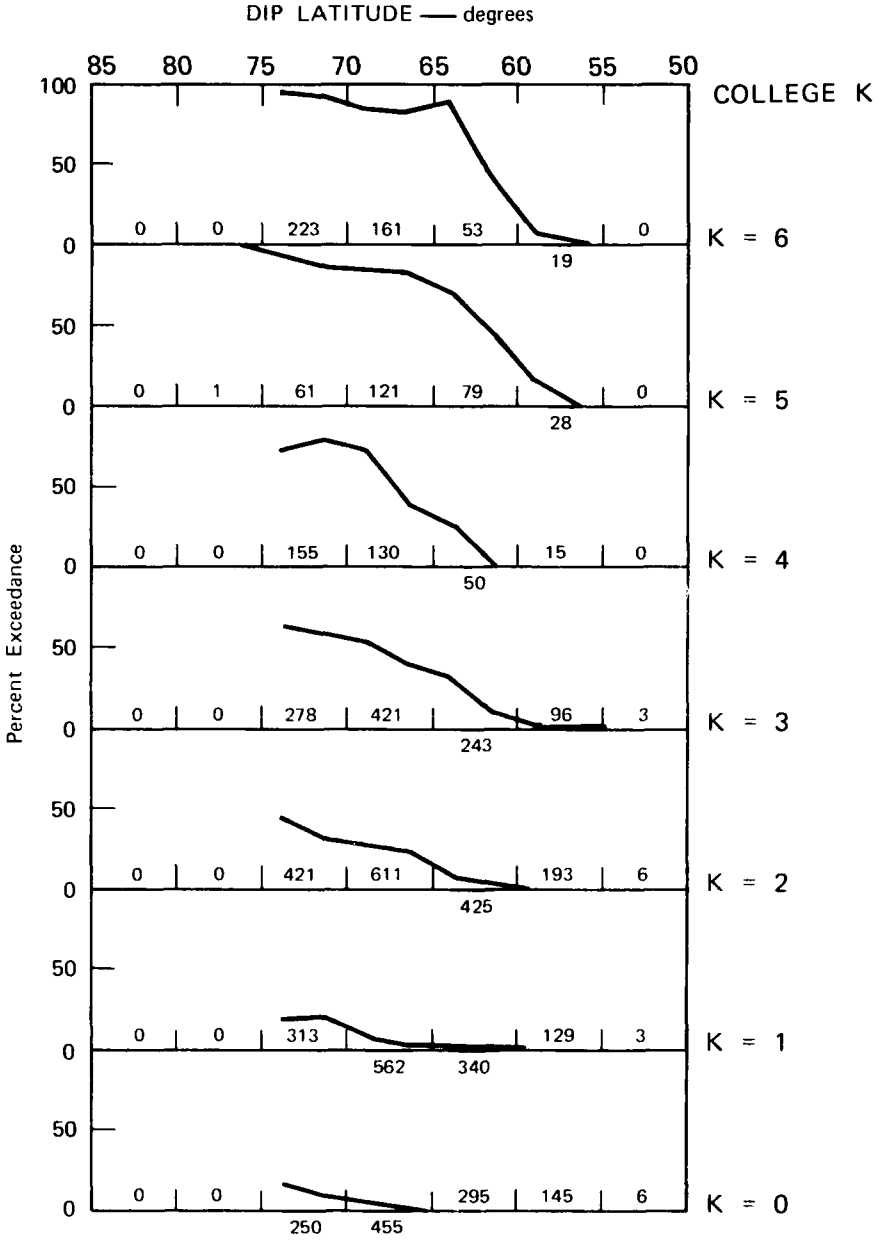

FIGURE 22 DEPENDENCE OF LATITUDINAL DISTRIBUTION OF DAYTIME σ_ϕ = 1 RADIAN EXCEEDANCE LEVEL ON LOCAL MAGNETIC ACTIVITY, 1977-1978 DATA

V GEOMETRICAL FACTORS INFLUENCING SCINTILLATION MORPHOLOGY

To model the geometrical factors that influence the latitudinal variation of scintillation activity, we have used the phase-screen theory developed in Rino and Matthews (1978) and Rino (1979). The measured phase variance is given by the formula

$$\langle \delta\phi^2 \rangle = \frac{2T}{p - 1} f_c^{1-p} \quad , \tag{1}$$

where f_c is the detrend cutoff frequency (0.1 Hz), p is the power-law index for the one-dimensional-phase spectral density, and

$$T = r_e^2 \lambda^2 \, (L \sec \theta) \, GC_s \frac{\sqrt{\pi}\, \Gamma(\nu)}{(2\pi)^{2\nu+1}\, \Gamma(\nu + 1/2)} v_{eff}^{2\nu-1} \quad . \tag{2}$$

The three-dimensional irregularity spectral density function is assumed to have the form $C_s q^{-(2\nu+1)}$, where $\nu = p/2$ and C_s is the "turbulent strength," which is easily related to the structure constant commonly used in characterizing turbulent fluids and plasmas. The T parameter itself is the turbulent strength for the one-dimensional temporal-phase power spectrum, which has the form Tf^{-p}.

The angle θ is the zenith angle and L sec θ is the length of the propagation path within the medium. The parameters r_e and λ are the classical electron radius and signal wavelength respectively. The main geometrical factors are G and v_{eff}. The former accounts for the "coherent" enhancement caused by the irregularity anisotropy. The "effective velocity" v_{eff} accommodates the space-to-time conversion, allowing for the aspect angle relative to the principal irregularity axis.

The anisotropy is characterized by the axial ratio along the magnetic field (a), and transverse to the magnetic field (b). In general,

the orientation angle of the second irregularity axis must be specified, but we shall consider only the sheet-like structures aligned along the local L shell--that is, transverse to the meridian plane. For a particular satellite pass, the anisotropy and height parameters are the principal variables. Since we have assumed a single layer; however, the LC_s value must be regarded as an effective or average value.

The weak scatter formula for S_4 corresponding to Eq. (1) is

$$S_4^2 = r_e^2 \lambda^2 \, (L \sec \theta) \, C_s Z^{\nu - 1/2} \left[\frac{\Gamma\left(\frac{2.5 - \nu}{2}\right)}{2\sqrt{\pi}\,\Gamma\left(\frac{\nu + 0.5}{2}\right)(\nu - 0.5)} \right] \mathfrak{J} \quad , \qquad (3)$$

where

$$Z = \frac{\lambda z_R \sec \theta}{4\pi} \quad , \qquad (4)$$

and $\mathfrak{J}$ is the geometrical enhancement factor for intensity corresponding to G. The parameter $\mathfrak{J}$, unlike G, depends on ν and is generally more complicated than G. In Eq. (4), z_R is the reduced range to the satellite.

Ideally, Eqs. (2) and (3) should be applied to each individual pass to determine the irregularity strength, which is independent of any purely geometrical factors. This procedure was applied to a limited number of data sets in Rino (1979). The scheme is not without pitfalls, however, and it is very time consuming. We have thus taken advantage of the similarity of the high-elevation passes and compared the summary statistics to calculations based on single passes.

In Figure 23 we show the amplitude and phase summary data for 1976-1977 (see Figures 11 and 12), together with model calculations for a post-midnight pass. A constant C_s level and a 100-km layer thickness were used. The C_s level was adjusted to match the phase-scintillation summary data at approximately 60° dip latitude.

The phase-scintillation data fit the model very well through the geometrical enhancement to $\approx 65°$ dip latitude. From that point poleward

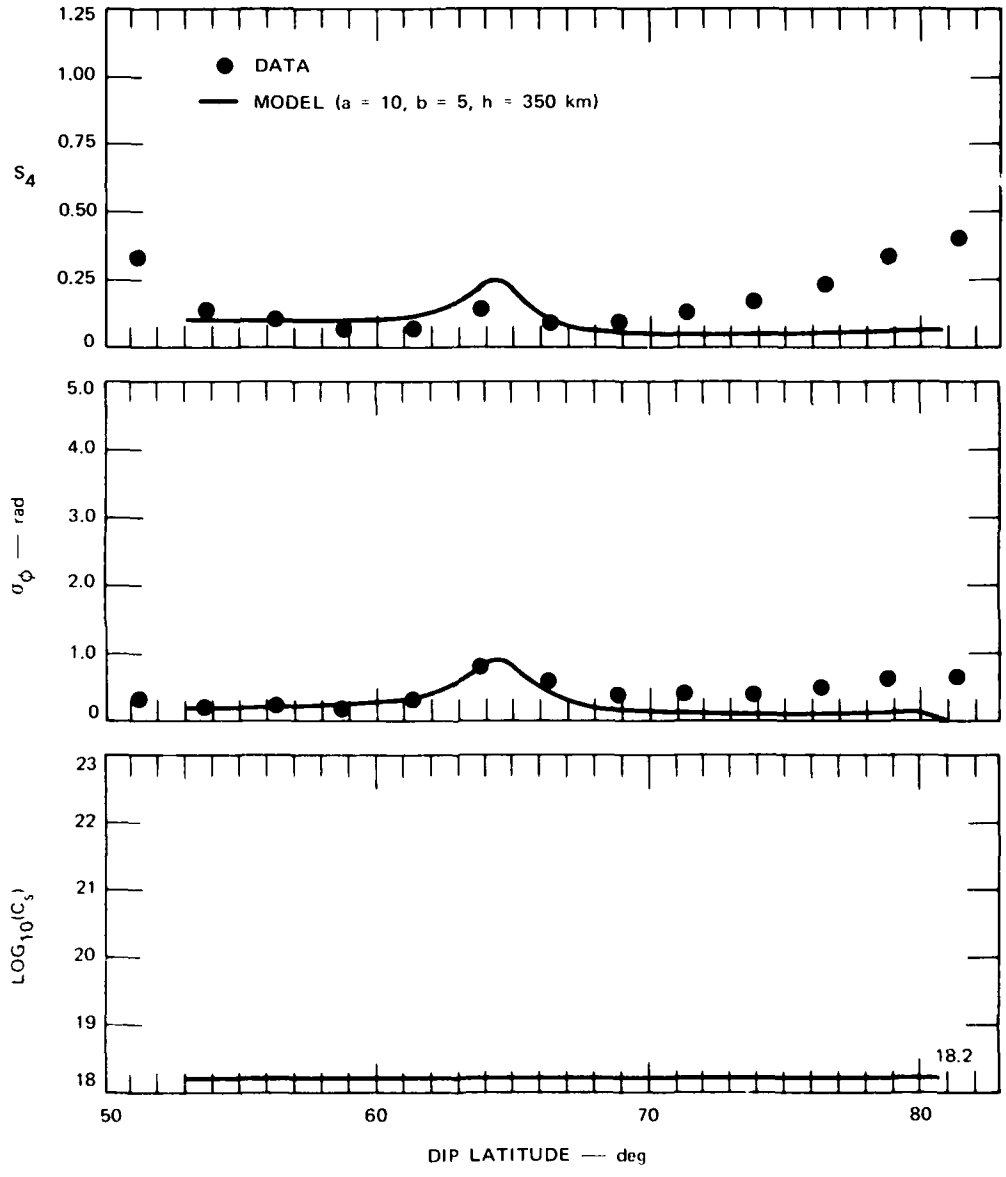

FIGURE 23 MODEL CALCULATIONS OF LATITUDINAL VARIATION OF S_4 AND σ_ϕ FOR LOW-ELEVATION PASS SUPERIMPOSED ON 50% EXCEEDANCE LEVELS FOR 1976-1977 DATA

there is a steadily increasing departure of the data from the theoretical curve based on a uniform perturbation level. We conclude that the general latitudinal distribution of auroral-zone structure has a monotonically increasing component beginning near the location of the midnight auroral oval ($\approx 65°$) under moderately disturbed conditions.

The corresponding theoretical S_4 curve overestimates the data from $\approx 60°$ through the region of the geometrical enhancement, and then underestimates the poleward data--as do the phase-variance calculations. Where the model overestimates the data, it is possibly because the multiple-scatter effects are neglected. As multiple-scatter effects are sensitive to anisotropy, saturation may well occur at lower turbulence levels, for propagation angles that intercept a major irregularity axis.

Alternatively, the discrepancy may indicate a contribution due to a source at higher altitudes. It can be seen from Eqs. (1) and (2) that a given turbulence level produces more phase scintillation when it is located at higher altitudes, because v_{eff} increases rapidly with altitude. A fixed phase scintillation level, alternatively, corresponds to less turbulence at high altitudes. In Eq. (3) the increase due to Z is overcome by the decrease in C_s, and S_4 actually decreases with increasing height if σ_ϕ is held constant. This is discussed in Rino (1979).

This is an attractive possibility, because there is mounting evidence that an F-region source often contributes to the purely geometrical enhancement caused by sheet-like irregularities. The evidence supporting this is from simultaneous two-station observations, and will be described in a separate report.

To address the question of how the averaging affects the data in Figure 24, we show the 1976-1977 data superimposed on model calculations for a high-elevation pass. The fit is generally poorer, particularly in the region of the geometrical enhancement. Since there are many more lower-elevation passes in the database than higher-elevation passes, this is not surprising. Ideally, one could weigh several geometries in

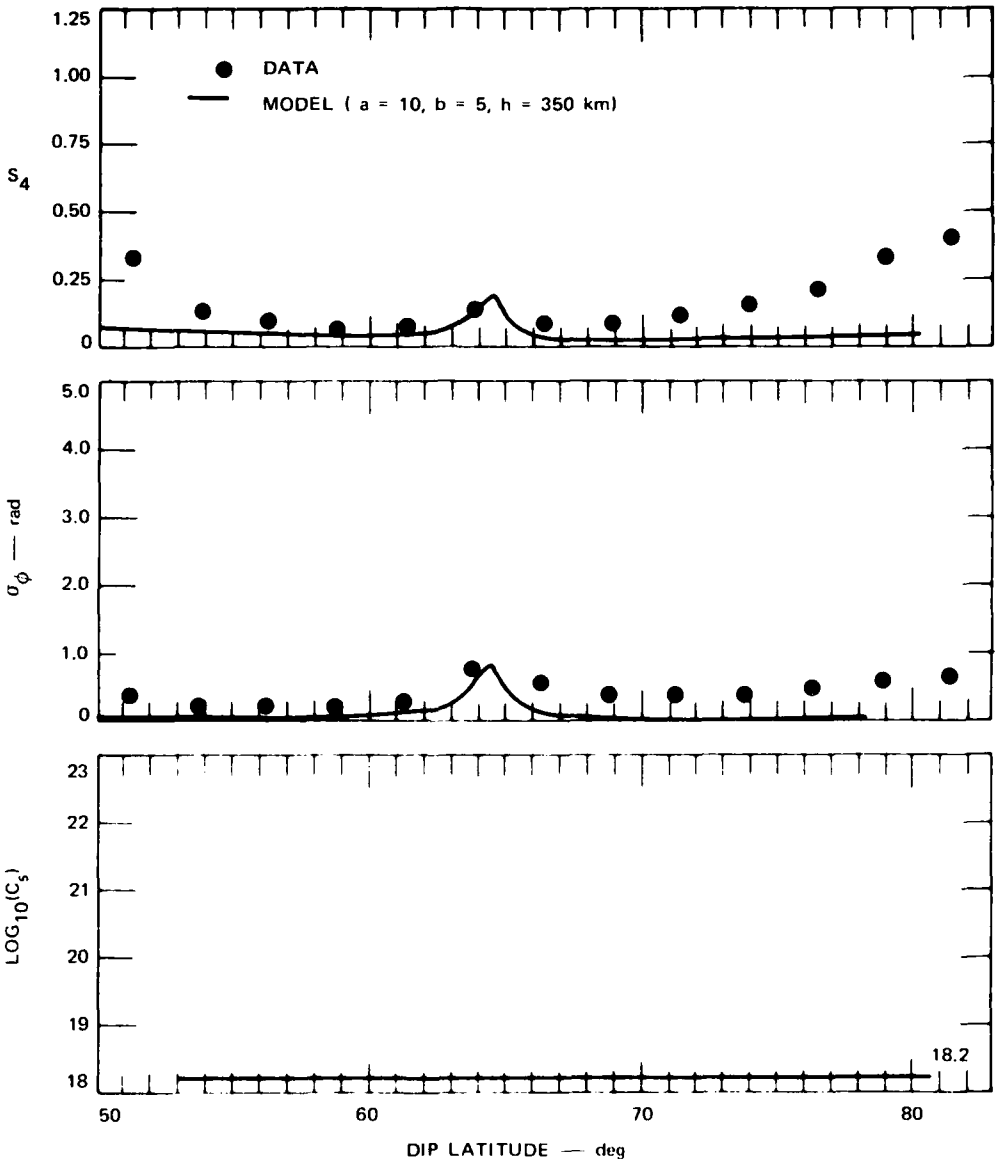

FIGURE 24 MODEL CALCULATIONS OF LATITUDINAL VARIATION OF S_4 AND σ_ϕ FOR HIGH-ELEVATION PASS SUPERIMPOSED ON 50% EXCEEDANCE LEVELS FOR 1976-1977 DATA

proportion to the pass distribution for similar maximum elevation angles, but this was not done.

The scintillation enhancement at ≈ 50° dip latitude has been discussed. If it is genuine and not just multipath contamination, it must be attributed to a subauroral source. Additional data have been recorded at Anchorage, Alaska, to study this feature, and we shall not pursue it further here.

In Figure 25, the summary data for 1977-1978 are shown together with model calculations of the average parameters. Here we see the same general features as were found in the 1976-1977 data. To fit the phase data at ≈ 60° dip latitude, however, it was necessary to increase $\log_{10} C_s$ from 18.2 to 18.5, which is small but significant.

The major difference in the two data-sets lies in the magnitude and rate of the increase, poleward, of 65°. The 1977-1978 data show a more rapid increase that starts within the region of the geometrical enhancement. This supports the hypothesis that a source region contributes to the geometrical enhancement. It also shows than an average increasing magnetic activity enhances the perturbation levels more than it moves boundary regions. The two effects are, however, difficult to separate.

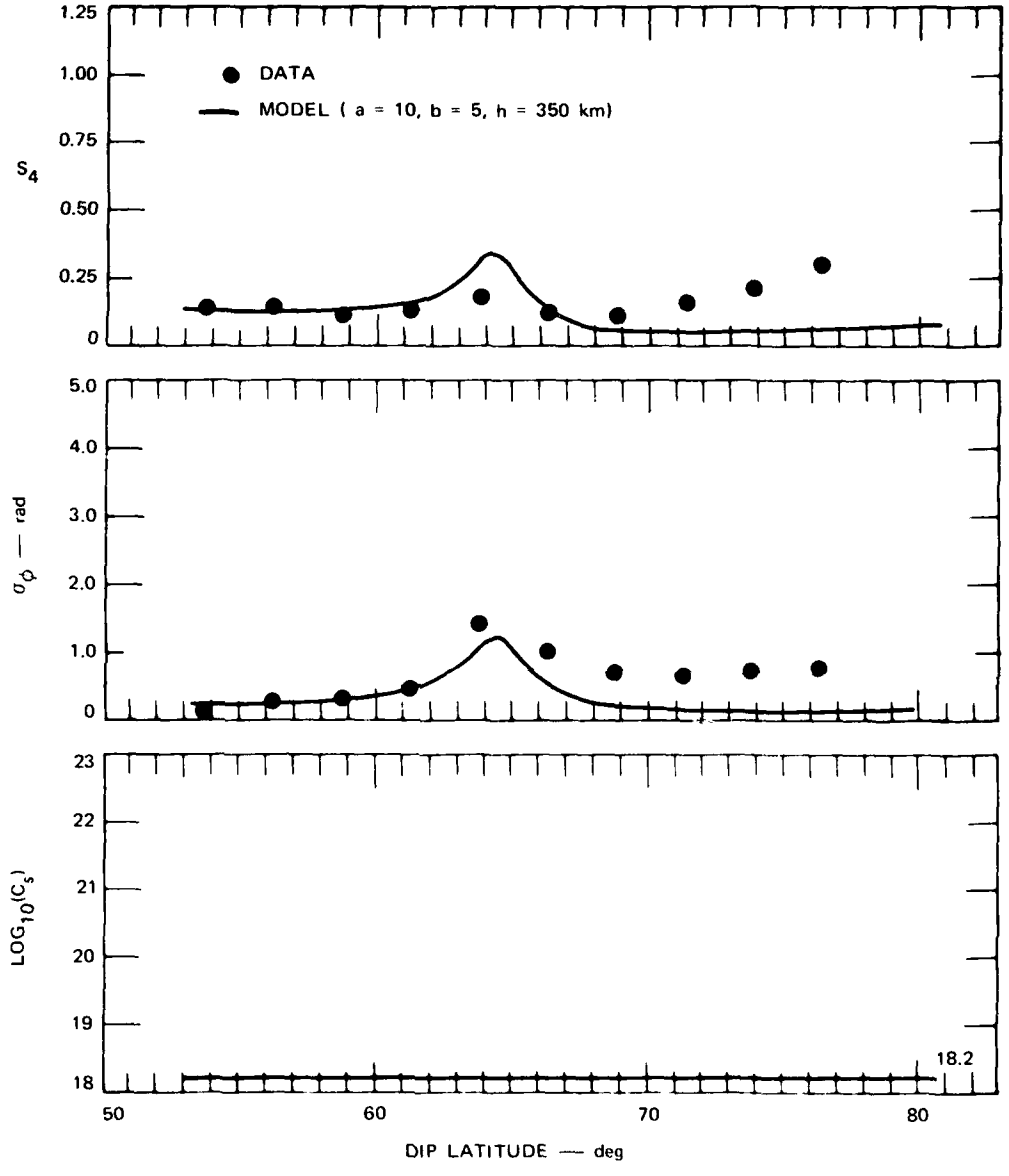

FIGURE 25 MODEL CALCULATIONS OF LATITUDINAL VARIATION OF S_4 AND σ_ϕ FOR LOW-ELEVATION PASS SUPERIMPOSED ON 50% EXCEEDANCE LEVELS FOR 1977-1978 DATA

REFERENCES

Aarons, J., "A Descriptive Model of F Layer High-Altitude Irregularities as Shown by Scintillation Observations," J. Geophys. Res., Vol. 78, No. 31, p. 7441, 1973.

Aarons, J., J. P. Mullen, and H. E. Whitney, "The Scintillation Boundary," J. Geophys. Res., Vol. 74, No. 3, p. 884, 1969.

Ahmed, M. and R. C. Sagalyn, "Topside Ionospheric Trough Morphology at Mid- and High-Latitudes," paper presented at the Symposium on the Effects of the Ionosphere on Space and Terrestrial Systems, January 24-26, 1978.

Basu, S., "Universal Time Seasonal Variations of Auroral Zone Magnetic Activity and VHF Scintillation," J. Geophys. Res., Vol. 80, No. 34, p. 4725, 1975.

Buchau, J., J. Aarons, J. P. Mullen, E. J. Weber, J. A. Whalen, H. E. Whitney, and E. E. Crampton, Jr., "Amplitude Scintillation Studies in the Polar Region on 250 MHz," paper presented at the Ionosphere Effects Symposium in Arlington, VA, January 24-26, 1978.

Fremouw, E. J., R. L. Leadabrand, R. C. Livingston, M. D. Cousins, C. L. Rino, B. C. Fair, and R. A. Long, "Early Results From the DNA Wideband Satellite Experiment--Complex-Signal Scintillation." Radio Science, Vol. 13, p. 167, 1978.

Martin, E. and J. Aarons, "F Layer Scintillations and the Aurora," J. Geophys. Res., Vol. 82, p. 2717, 1977.

Phelps, A.D.R. and R. C. Sagalyn, "Plasma Density Irregularities in the High-Latitude Top Side Ionosphere," J. Geophys. Res., Vol. 81, No. 4, p. 515, 1976.

Rino, C. L., "A Power-Law Phase Screen Model for Ionospheric Scintillation 1. Weak Scatter," in press, Radio Science, 1979.

Rino, C. L. and S. J. Matthews, "On the Interpretation of Ionospheric Scintillation Data Using a Power-Law Phase-Screen Model--Weak Scatter," DNA 4606T, Topical Report 2, Contract DNA001-77-C-0220, SRI Project 6434, SRI International, Menlo Park, CA, 1978.

Rino, C. L., R. C. Livingston, and S. J. Matthews, "Evidence for Sheet-Like Auroral Ionospheric Irregularities," Geophys. Res. Letts., Vol. 5, No. 12, p. 1039, 1978.

Sagalyn, R. C. and M. Smiddy, "High-Latitude Irregularities in the Top Side Ionosphere Based on ISIS 1 Thermal Probe Data," J. Geophys. Res., Vol. 79, No. 28, p. 4252, 1974.

DISTRIBUTION LIST

DEPARTMENT OF DEFENSE

Assistant Secretary of Defense
Comm., Cmd., Cont. & Intell.
ATTN: Dir. of Intelligence Systems, J. Babcock
ATTN: C3IST&CCS, M. Epstein

Assistant to the Secretary of Defense
Atomic Energy
ATTN: Executive Assistant

Command & Control Technical Center
ATTN: C-650, G. Jones
ATTN: C-312, R. Mason
3 cy ATTN: C-650, W. Heidig

Defense Advanced Rsch. Proj. Agency
ATTN: TIO

Defense Communications Agency
ATTN: Code 810, J. Barna
ATTN: Code 205
ATTN: Code 101B
ATTN: Code 480
ATTN: Code R1033, M. Raffensperger
ATTN: Code 480, F. Dieter

Defense Communications Engineer Center
ATTN: Code R123
ATTN: Code R410, R. Craighill
ATTN: Code R720, J. Worthington
ATTN: Code R410, J. McLean

Defense Intelligence Agency
ATTN: DT-1B
ATTN: DB-4C, E. O'Farrell
ATTN: DT-5
ATTN: DB, A. Wise
ATTN: DC-7D, W. Wittig
ATTN: HQ-TR, J. Stewart

Defense Nuclear Agency
ATTN: STVL
3 cy ATTN: RAAE
4 cy ATTN: TITL

Defense Technical Information Center
12 cy ATTN: DD

Field Command
Defense Nuclear Agency
ATTN: FCPR

Field Command
Defense Nuclear Agency
Livermore Division
ATTN: FCPRL

Interservice Nuclear Weapons School
ATTN: TTV

Joint Chiefs of Staff
ATTN: C3S
ATTN: C3S, Evaluation Office

DEPARTMENT OF DEFENSE (Continued)

Joint Strat. Tgt. Planning Staff
ATTN: JLA
ATTN: JLTW-2

National Security Agency
ATTN: B-3, F. Leonard
ATTN: W-32, O. Bartlett
ATTN: R-52, J. Skillman

Undersecretary of Defense for Rsch. & Engrg.
ATTN: Strategic & Space Systems (OS)

WWMCCS System Engineering Org.
ATTN: J. Hoff
ATTN: R. Crawford

DEPARTMENT OF THE ARMY

Assistant Chief of Staff for Automation & Comm.
Department of the Army
ATTN: DAAC-ZT, P. Kenny

Atmospheric Sciences Laboratory
U.S. Army Electronics R & D Command
ATTN: DELAS-EO, F. Niles

BMD Systems Command
Department of the Army
2 cy ATTN: BMDSC-HW

Deputy Chief of Staff for Ops. & Plans
Department of the Army
ATTN: DAMO-RQC

Electronics Tech. & Devices Lab.
Department of the Army
ATTN: DELET-ER, H. Bomke

Harry Diamond Laboratories
Department of the Army
ATTN: DELHD-I-TL, M. Weiner
ATTN: DELHD-N-P
ATTN: DELHD-N-RB, R. Williams
ATTN: DELHD-N-P, F. Wimenitz

U.S. Army Comm.-Elec. Engrg. Instal. Agency
ATTN: CCC-EMEO-PED, G. Lane
ATTN: CCC-CED-CCO, W. Neuendorf
ATTN: CCC-EMEO, W. Nair

U.S. Army Communications Command
ATTN: CC-OPS-W
ATTN: CC-OPS-WR, H. Wilson

U.S. Army Communications R&D Command
ATTN: DRDCO-COM-RY, W. Kesselman

U.S. Army Foreign Science & Tech. Ctr.
ATTN: DRXST-SD

U.S. Army Materiel Dev. & Readiness Cmd.
ATTN: DRCLDC, J. Bender

DEPARTMENT OF THE ARMY (Continued)

U.S. Army Nuclear & Chemical Agency
ATTN: Library

U.S. Army Satellite Comm. Agency
ATTN: Document Control

U.S. Army TRADOC Systems Analysis Activity
ATTN: ATAA-PL
ATTN: ATAA-TDC
ATTN: ATAA-TCC, F. Payan, Jr.

DEPARTMENT OF THE NAVY

Joint Cruise Missile Project Office
Department of the Navy
ATTN: JCM-G-70

Naval Air Development Center
ATTN: Code 6091, M. Setz

Naval Air Systems Command
ATTN: PMA 271

Naval Electronic Systems Command
ATTN: PME 117-211, B. Kruger
ATTN: PME 106-4, S. Kearney
ATTN: PME 117-20
ATTN: PME 106-13, T. Griffin
ATTN: Code 3101, T. Hughes
ATTN: Code 501A
ATTN: PME 117-2013, G. Burnhart

Naval Intelligence Support Ctr.
ATTN: NISC-50

Naval Ocean Systems Center
ATTN: Code 5322, M. Paulson
ATTN: Code 532, J. Bickel
3 cy ATTN: Code 5324, W. Moler

Naval Research Laboratory
ATTN: Code 6780, S. Ossakow
ATTN: Code 6700, T. Coffey
ATTN: Code 7500, B. Wald
ATTN: Code 7550, J. Davis

Naval Space Surveillance System
ATTN: J. Burton

Naval Surface Weapons Center
ATTN: Code F31

Naval Surface Weapons Center
ATTN: Code F-14, R. Butler

Naval Telecommunications Command
ATTN: Code 341

Office of Naval Research
ATTN: Code 421
ATTN: Code 420

Office of the Chief of Naval Operations
ATTN: OP 604C
ATTN: OP 981N
ATTN: OP 941D

DEPARTMENT OF THE NAVY (Continued)

Strategic Systems Project Office
Department of the Navy
ATTN: NSP-43
ATTN: NSP-2722, F. Wimberly
ATTN: NSP-2141

DEPARTMENT OF THE AIR FORCE

Aerospace Defense Command
Department of the Air Force
ATTN: DC, T. Long

Air Force Avionics Laboratory
ATTN: AAD, W. Hunt
ATTN: AAD, A. Johnson

Air Force Geophysics Laboratory
ATTN: LKB, K. Champion
ATTN: OPR-1, J. Ulwick
ATTN: PHP, J. Mullen
ATTN: OPR, A. Stair
ATTN: PHP, J. Aarons
ATTN: PHI, J. Buchau

Air Force Weapons Laboratory
Air Force Systems Command
ATTN: SUL
ATTN: DYC

Air Logistics Command
Department of the Air Force
ATTN: OO-ALC/MM, R. Blackburn

Assistant Chief of Staff
Intelligence
Department of the Air Force
ATTN: INED

Assistant Chief of Staff
Studies & Analyses
Department of the Air Force
ATTN: AF/SASC, W. Adams
ATTN: AF/SASC, G. Zank

Ballistic Missile Office
Air Force Systems Command
ATTN: MNNH
ATTN: MNNH, M. Baran
ATTN: MNNL, S. Kennedy

Deputy Chief of Staff
Operations Plans and Readiness
Department of the Air Force
ATTN: AFXOKCD
ATTN: AFXOXFD
ATTN: AFXOKS
ATTN: AFXOKT

Deputy Chief of Staff
Research, Development, & Acq.
Department of the Air Force
ATTN: AFRDSP
ATTN: AFRDS
ATTN: AFRDQ
ATTN: AFRDSS

DEPARTMENT OF THE AIR FORCE (Continued)

Electronic Systems Division
Department of the Air Force
ATTN: DCKC, J. Clark

Electronic Systems Division
Department of the Air Force
ATTN: XRW, J. Deas

Electronic Systems Division
Department of the Air Force
ATTN: YSM, J. Kobelski
ATTN: YSEA

Foreign Technology Division
Air Force Systems Command
ATTN: NIIS, Library
ATTN: TQTD, B. Ballard
ATTN: SDEC, A. Oakes

Headquarters Space Division
Air Force Systems Command
ATTN: SKA, M. Clavin
ATTN: SKA, C. Rightmyer

Headquarters Space Division
Air Force Systems Command
ATTN: SZJ, W. Mercer
ATTN: SZJ, L. Doan

Rome Air Development Center
Air Force Systems Command
ATTN: TSLD
ATTN: OCS, V. Coyne

Rome Air Development Center
Air Force Systems Command
ATTN: EEP

Strategic Air Command
Department of the Air Force
ATTN: XPFS
ATTN: DCXF
ATTN: DCXT, T. Jorgensen
ATTN: NRT
ATTN: DCXT
ATTN: DCX
ATTN: OOKSN

DEPARTMENT OF ENERGY CONTRACTORS

EG&G, Inc.
Los Alamos Division
ATTN: J. Colvin
ATTN: D. Wright

Lawrence Livermore Laboratory
ATTN: Technical Information Dept. Library

Los Alamos Scientific Laboratory
ATTN: R. Taschek
ATTN: D. Westervelt
ATTN: P. Keaton

Sandia Laboratories
Livermore Laboratory
ATTN: B. Murphey
ATTN: T. Cook

DEPARTMENT OF ENERGY CONTRACTORS (Continued)

Sandia Laboratories
ATTN: D. Thornbrough
ATTN: Org. 1250, W. Brown
ATTN: 3141
ATTN: Space Project Div.
ATTN: D. Dahlgren

OTHER GOVERNMENT AGENCIES

Central Intelligence Agency
ATTN: OSI/PSTD

Department of Commerce
National Bureau of Standards
ATTN: Sec. Officer for R. Moore

Department of Commerce
National Oceanic & Atmospheric Admin.
ATTN: R. Grubb

Institute for Telecommunications Sciences
National Telecommunications & Info Admin.
ATTN: A. Jean
ATTN: W. Utlaut
ATTN: D. Crombie
ATTN: L. Berry

U.S. Coast Guard
Department of Transportation
ATTN: G-DOE-3/TP54, B. Romine

DEPARTMENT OF DEFENSE CONTRACTORS

Aerospace Corp.
ATTN: N. Stockwell
ATTN: T. Salmi
ATTN: F. Morse
ATTN: I. Garfunkel
ATTN: V. Josephson
ATTN: R. Slaughter
ATTN: D. Olsen
ATTN: S. Bower

University of Alaska
ATTN: T. Davis
ATTN: Technical Library
ATTN: N. Brown

Analytical Systems Engineering Corp.
ATTN: Radio Sciences

Analytical Systems Engineering Corp.
ATTN: Security

Barry Research Communications
ATTN: J. McLaughlin

BDM Corp.
ATTN: T. Jacobs
ATTN: T. Neighbors

Berkeley Research Associates, Inc.
ATTN: J. Workman

Boeing Co.
ATTN: S. Tashird
ATTN: M/S 42-33, J. Kennedy
ATTN: G. Hall

DEPARTMENT OF DEFENSE CONTRACTORS (Continued)

University of California at San Diego
ATTN: H. Booker

Charles Stark Draper Lab., Inc.
ATTN: J. Gilmore
ATTN: D. Cox

Computer Sciences Corp.
ATTN: H. Blank

Comsat Labs.
ATTN: G. Hyde
ATTN: R. Taur

Cornell University
ATTN: D. Farley, Jr.

Electrospace Systems, Inc.
ATTN: H. Logston

ESL, Inc.
ATTN: J. Roberts
ATTN: C. Prettie
ATTN: J. Marshall

Ford Aerospace & Communications Corp.
ATTN: J. Mattingley

General Electric Co.
ATTN: M. Bortner

General Electric Co.
ATTN: C. Zierdt
ATTN: A. Steinmayer
ATTN: S. Lipson

General Electric Co.
ATTN: F. Reibert

General Electric Company—TEMPO
ATTN: D. Chandler
ATTN: DASIAC
ATTN: T. Stevens
ATTN: M. Stanton
ATTN: W. Knapp

General Electric Tech. Services Co., Inc.
ATTN: G. Millman

General Research Corp.
ATTN: J. Ise, Jr.
ATTN: J. Garbarino

GTE Sylvania, Inc.
ATTN: M. Cross

[illegible], Inc.
ATTN: D. Hansen

IBM Corp.
ATTN: F. Ricci

University of Illinois
ATTN: Security Supervisor for K. Yeh

Institute for Defense Analyses
ATTN: J. Aein
ATTN: E. Bauer
ATTN: J. Bengston
ATTN: H. Wolfhard

DEPARTMENT OF DEFENSE CONTRACTORS (Continued)

International Tel. & Telegraph Corp.
ATTN: G. Wetmore
ATTN: Technical Library

JAYCOR
ATTN: S. Goldman

JAYCOR
ATTN: D. Carlos

Johns Hopkins University
ATTN: T. Potemra
ATTN: Document Librarian
ATTN: T. Evans
ATTN: J. Newland
ATTN: P. Komiske
ATTN: B. Wise

Kaman Sciences Corp.
ATTN: T. Meagher

Linkabit Corp.
ATTN: I. Jacobs

Litton Systems, Inc.
ATTN: R. Grasty

Lockheed Missiles & Space Co., Inc.
ATTN: M. Walt
ATTN: R. Johnson
ATTN: W. Imhof

Lockheed Missiles & Space Co., Inc.
ATTN: Dept. 60-12
ATTN: D. Churchill

M.I.T. Lincoln Lab.
ATTN: D. Towle
ATTN: L. Loughlin

McDonnell Douglas Corp.
ATTN: J. Moule
ATTN: W. Olson
ATTN: G. Mroz
ATTN: N. Harris

Meteor Communications Consultants
ATTN: R. Leader

Mission Research Corp.
ATTN: R. Bogusch
ATTN: S. Gutsche
ATTN: D. Sowle
ATTN: F. Fajen
ATTN: R. Hendrick

Mitre Corp.
ATTN: C. Callahan
ATTN: A. Kymmel
ATTN: B. Adams
ATTN: G. Harding

Mitre Corp.
ATTN: W. Foster
ATTN: M. Horrocks
ATTN: W. Hall

Pacific-Sierra Research Corp.
ATTN: E. Field, Jr.

DEPARTMENT OF DEFENSE CONTRACTORS (Continued)

Pennsylvania State University
ATTN: Ionospheric Research Lab.

Photometrics, Inc.
ATTN: I. Kofsky

Physical Dynamics, Inc.
ATTN: E. Fremouw

R & D Associates
ATTN: W. Karzas
ATTN: B. Gabbard
ATTN: R. Lelevier
ATTN: R. Turco
ATTN: F. Gilmore
ATTN: C. Greifinger
ATTN: C. MacDonald
ATTN: W. Wright, Jr.
ATTN: M. Gantsweg
ATTN: H. Ory

R & D Associates
ATTN: L. Delaney
ATTN: B. Yoon

Rand Corp.
ATTN: C. Crain
ATTN: E. Bedrozian

Riverside Research Institute
ATTN: V. Trapani

Rockwell International Corp.
ATTN: J. Kristof

Santa Fe Corp.
ATTN: E. Ortlieb

Science Applications, Inc.
ATTN: D. Divis

DEPARTMENT OF DEFENSE CONTRACTORS (Continued)

Science Applications, Inc.
ATTN: J. McDougall
ATTN: E. Straker
ATTN: L. Linson
ATTN: D. Sachs
ATTN: C. Smith
ATTN: D. Hamlin

Science Applications, Inc.
ATTN: SZ

SRI International
ATTN: R. Livingston
ATTN: W. Chesnut
ATTN: W. Jaye
ATTN: C. Rino
ATTN: G. Smith
ATTN: A. Burns
ATTN: M. Baron
ATTN: D. Neilson
ATTN: R. Leadabrand
ATTN: G. Price

Teledyne Brown Engineering
ATTN: R. Deliberis

Tri-Com, Inc.
ATTN: D. Murray

TRW Defense & Space Sys. Group
ATTN: R. Plebuch
ATTN: D. Dee
ATTN: S. Altschuler

Utah State University
ATTN: L. Jensen
ATTN: K. Baker

Visidyne, Inc.
ATTN: J. Carpenter